6-2011

Electrochemistry of technetium analogues rhenium and molybdenum in room temperature ionic liquid

Pauline Nancy Serrano
University of Nevada, Las Vegas

ELECTROCHEMISTRY OF TECHNETIUM ANALOGUES RHENIUM AND MOLYBDENUM IN ROOM TEMPERATURE IONIC LIQUID

by

Pauline Nancy Serrano

Bachelor of Science
University of Nevada, Las Vegas
2005

A thesis submitted in partial fulfillment
of the requirements for the

Master of Science in Chemistry Degree
Department of Chemistry
College of Sciences

Graduate College
University of Nevada, Las Vegas
June 2011

THE GRADUATE COLLEGE

We recommend the thesis prepared under our supervision by

Pauline Nancy Serrano

entitled

Electrochemistry of Technetium Analogues Rhenium and Molybdenum in Room Temperature Ionic Liquid

be accepted in partial fulfillment of the requirements for the degree of

Master of Science in Chemistry
Department of Chemistry

David Hatchett, Committee Chair

Dong Chan Lee, Committee Member

Patricia Paviet-Hartman, Committee Member

Jacimaria Batista, Graduate College Representative

Ronald Smith, Ph. D., Vice President for Research and Graduate Studies
and Dean of the Graduate College

August 2011

ABSTRACT

Electrochemistry of Technetium Analogs Rhenium and Molybdenum in Room Temperature Ionic Liquid

by

Pauline N. Serrano

Dr. David Hatchett, Examination Committee Chair
Professor of Analytical Chemistry
University of Nevada, Las Vegas

Rhenium was used as an analog for Technetium to study the electrochemical redox properties because the two elements share the same stable oxidation states in aqueous solutions. However, Tc-99 is radioactive and is not readily available for experimentation purposes. Molybdenum is also of interest because when Mo-99 is irradiated, the decay products are Tc-99m and Tc-99. Approximately 30% Tc-99m is eluted from the Mo columns for radiopharmaceutical use with the remaining Mo-99 source decaying to Tc-99 which is discarded as radioactive hospital waste. Currently there are no viable procedures for the reclamation of the radioactive Tc-99 from either fission streams or from the hospital waste. Investigating the electrochemical properties of Re and Mo are important for developing methodologies to increase the percent elution of Tc-99m, and ultimately improve reclamation procedures of the waste Tc-99. In this study RTIL solutions are utilized in place of aqueous solutions for the electrochemical analysis and deposition of both Re and Mo. In these studies the RTIL was used to eliminate the competitive side reactions associated with water, remove the acid dependence associated with the reduction of Re and Mo species, and extend the negative potential window such that reduction of the species to metal was achieved. The electrochemical and SEM results indicate that Re and Mo were reduced and deposited

onto working electrodes. With the growing stores of hazardous technetium from the medical industry and nuclear fuel reprocessing, mechanisms for deposition and recovery are increasingly important. The studies outlined in this thesis defense increase our understanding of the electrochemistry of stable analogues, Re and Mo and in turn increase our understanding suggesting that the target recovery of Tc can be achieved using RTIL solutions.

ACKNOWLEDGEMENTS

I would like to thank my thesis committee for your help in producing my final thesis document for my master's degree in chemistry. Dr. Lee I have appreciated all your feedback and commitment to academia in this setting and also as a professor in my advanced chemistry courses. Your expectations of your students are helping make University of Nevada, Las Vegas a better institution of higher learning. Dr. Paviet-Hartmann your expertise and enthusiasm of industrial radiochemistry have given me the tools needed to understand wholly the outcome of my work. Dr. Batista your outside perspective of my work was an integral part of my comprehensive thesis. Thank you for your time, while working on my thesis.

David Hatchett I cannot fully express the depth of my appreciation of your mentorship and guidance over the course of the last 8 years. As undergraduate you challenged me to become a free thinking scientist. Further, by allowing me to join your research group for my master's opened the door for alternative route for my future, changing my life forever. Your guidance in my academic career led to pursue a doctoral degree, and when I doubted myself, you were always there to reassure me that I was indeed capable of great things.

I would like to thank my research group for the lab support and positive feedback. Dr. John Kinyanjui for your years of dedication and for passing on invaluable knowledge, there were many times I'm not sure I would have succeeded without you. To Jade Morgan thanks for all of the laughs and cups of coffee during the long hours in lab. Also for all of the night caps after long work hours, the lab was never the same without you. Thank you Tam Quy for your help during our course work, because I'm pretty sure I still

don’t know how to use MathCad. I would also like to acknowledge Janelle Droessler, the newest member to the research group. You are going to make a great scientist and I look forward to great thing you will achieve. Also, I would like to acknowledge the undergraduates who helped in during a very critical time of my research, Pavlin Dimitrov for your incredible data processing skills and dedication to having reproducible results. To my last two undergraduate research assistants: Jamie MacAchor and Winnie David for working with me around the clock to gather the necessary data to finish my thesis in time. Thank you for your suggestions and feedback. .

To my graduate student peers and friends, thank you for always sharing your enthusiasm for learning and lending an ear when needed. Michael Hand, thank you for your support and patience every single day. Your enthusiasm for life and light heartedness brings so much joy to my life, I am ever grateful for having you in my life.

Finally I would like to dedicate my thesis to my family for always believing in me, when I couldn’t even comprehend it. To my parents who sacrificed so much to help me through my seemingly endless education. Specifically I would like to thank my mother, Adeline because through her actions I learned that women can be strong, independent, and smart. She taught me invaluable lessons about believing in myself and that through dedication and hard work anything can be achieved. Also, to my father, Eusebio who sacrificed so much by coming to this country at the age of 15 and endured many hardships to provide for our family. You instilled an incredible work ethic and a dedication to excellence. To my older sister Edith, you always had our family’s needs before her own and taking great care of me. You always made sure that I was fed and hydrated through the vigorous writing process. To my younger sister, you were always

eager to learn about science (genes vs. jeans) and willing to lend a helping hand whenever I needed it. Your light hearted ways seemed to lighten the mood when I needed it the most. I would also like to extend a thanks to my extended family; Dr. Jeffrey Wagner. Thank you for your help and input at a very critical time during my thesis writing campaign. Your tough love always seems to have the most appropriate timing. To my wonderful niece, Amelia I appreciate your smiles and laughs more than you could ever know. I hope to be a role model in your life that you can look up to.

TABLE OF CONTENTS

LIST OF TABLES

LIST OF FIGURES

CHAPTER 1

INTRODUCTION

1.1 Background and PUREX Process

The PUREX (Plutonium/Uranium Extraction) process is the industrial procedure for recycling used nuclear fuel (UNF), where fission products are removed and useable uranium (U(VI)) and plutonium (Pu(IV)) are then recovered [1-4]. At the beginning of the PUREX process the used fuel is chopped into small pieces and dissolved in 3 M – 4 M nitric acid. Once fully dissolved, the uranium and plutonium species are extracted by 30% tri-n-butyl-phosphate (TBP) dissolved into 70% dodecane (or kerosene). U(VI) and Pu(IV) are separated as $UO_2(NO_3)_2.2TBP$ and $Pu(NO_3)_4.2TBP$ from the raffinate containing all the fission products and purified in multi-stage extraction cycles. The remaining liquid after plutonium and uranium removed is high-level waste, containing about 3% of used fuel in the form of fission products and minor actinides [5]. It is highly radioactive and generates a significant amount of heat.

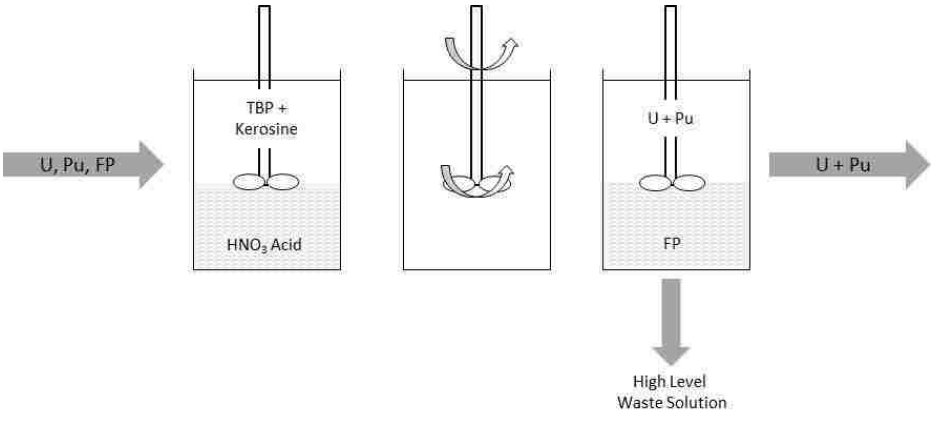

Figure 1.1: Extraction Principle for PUREX [6]

Due to the specific nature of the extractant TBP, species such as Strontium (Sr-90), Cesium (Cs-137), and Technetium (Tc-99) are not extracted and remain in the first aqueous raffinate. The raffinate is the liquid stream, which remains after the extraction with the immiscible liquid, removes solutes from the original liquor. The small activity of Tc-99 relative to other fission products, like Cs-137 or Sr-90, and its long half-life ($t_{1/2}$ = 2.1 x 10^5 years), makes it one of the key isotopes for analysis in radioactive liquid waste streams for reprocessing industry [3, 4]. The presence of Tc-99 in real effluent is problematic because it favors its more thermodynamically stable anionic form, pertechnetate TcO_4^-, which is highly mobile species, making it challenging for safe disposal.

Currently methods to directly separate Tc-99 from the PUREX process are still in the R&D mode because of the nature of the extractant as well as the medium [7-9]. A promising method for the separation and recovery of Tc-99 is based on the potential dependent electrochemical deposition of technetium from the reprocessing solution targeting TcO_4^-. Alternatively the extraction of TcO_4^- into room temperature ionic liquid (RTIL) can be envisioned for electrochemical recovery from non-aqueous environments. Room temperature ionic liquid can be defined as a molten salt that is liquid at low temperatures, wholly composed of ions [10-12]. This may be accomplished by mixing known amounts of TcO_4^-, which is already dissolved in HNO_3, into acidified RTIL [13-15]. The interactions between the cations of the RTIL and the TcO_4^- allow for solvation. This mixture separates and the RTIL remains intact. This process can also be used with similar species such as ReO_4^-, MoO_2, and MoO_4^{2-}. Reclamation from aqueous or non-aqueous solutions using electrochemical methods is an attractive method because it is

clean, efficient, and inexpensive relative to using other extraction methods. RTIL may also be envisioned as a complementary technique for new advanced separation technologies such as the COEX^{TM}(co-extraction) process where U(VI) and Pu(IV) are co-extracted by 30% tri-n-butylphosphate, 70% dodecane and co-precipitated as a mixed oxide (MOX) fuel$(Pu,U)O_2$ [16, 17].MOX fuel is a nuclear fuel that contains more than one oxide or fissile materials. Usually referring to a blend of oxides of plutonium and natural uranium, reprocessed uranium, or depleted uranium, which behave similarly to low enriched uranium (LEU) oxide fuel. MOX fuel is an alternative to LEU fuel used in light water reactors. The precipitation of U(VI) or Pu(IV) or both is performed by adding oxalic acid to the solution, resulting in an oxalate precipitate. This precipitate is calcinated to 400^{o}C – 600^{o}C to form MOX.

The PUREX process was originally designed to purify plutonium for weapon purposes the COEX process (co-extraction) does not separate pure plutonium at any point in the recycling plant [18].

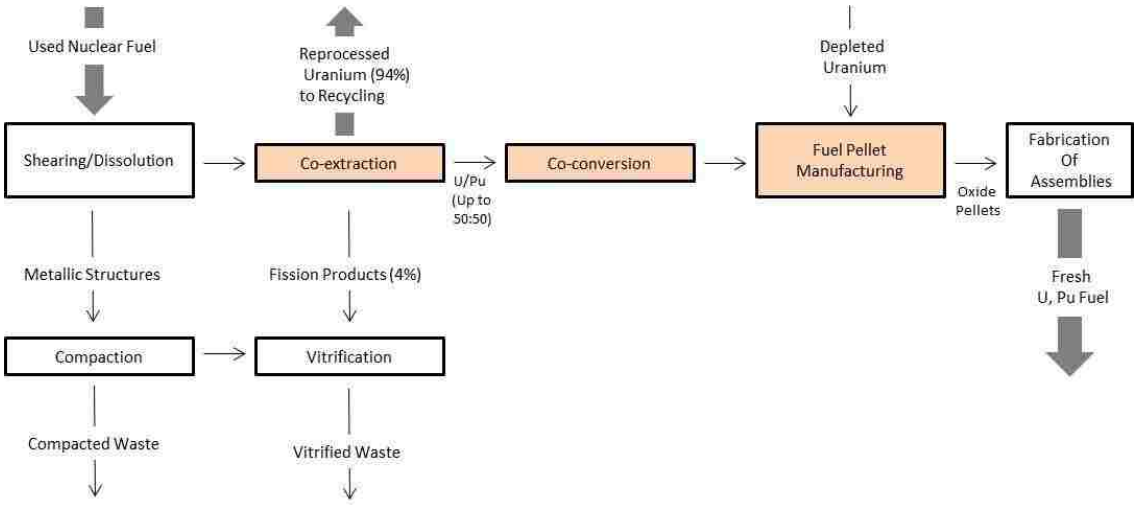

Figure 1.2: Proposed Recycling at AREVA Based on a New Integrated Co-extraction (COEX) Process [19]

An additional attraction of MOX fuel is that it provides a way to dispose of surplus weapon grade plutonium in the current U.S. fleet of conventional light water reactors (LWR's). It is conditioned by calcining and incorporating the dry material into vitrified solid, pending for disposal [19, 20].

1.1.1 Technetium

Tc-99 is unstable and only minute traces occur as a spontaneous fission product in uranium ores [21, 22]. Among the long-lived technetium isotope the only beta emitter is Tc-99 and it is obtained in small amounts either by extended neutron irradiation of highly purified molybdenum or by induced fission of U-235, making it the most common and most readily available Tc isotope (others include Tc-98 and Tc-97). A kilogram of uranium contains an estimated 1 nanogram of technetium [23]. The fission of a gram of U-235 in nuclear reactors yields 27mg of Tc-99[23]. Other fissile isotopes also produce similar yields of Tc, 4.9% from U-233 and 6.21% Pu-239 [23].

The long half-life of Tc-99and its ability to form anionic species such as TcO_4^- makes it a major concern for long-term disposal of radioactive waste and separation [24]. Many of the processes designed to remove fission products in reprocessing plants target cationic species that do not favor the retention of Tc in the treatment process. Current French and Japanese disposal favors burial of the waste encapsulated in glass designed for deep, underground repositories or in geologically stable rock. Therefore, the use of anionic forms of high activity fission materials such as TcO_4^- is problematic in current disposal

processes. In a dry repository there are no expected chemical changes to the glass waste, because no oxidizing agents can be found. However, if the container encounters any contact with aqueous environmental solutions the vitrified waste may be altered by initiating chemical reactions depending on the composition of the solution, pH, redox potential, and temperature. In the presence of water and oxygen, TcO_2 will be readily oxidized to soluble TcO_4^-.

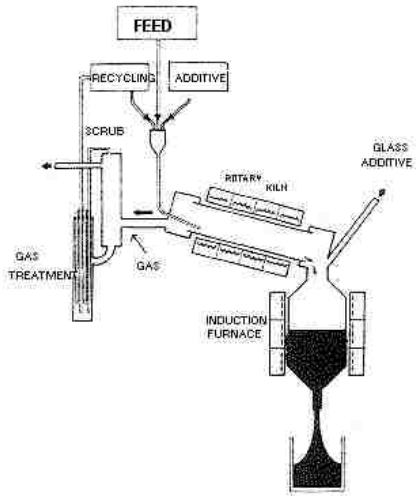

Figure 1.3: Vitrification of Raffinate [6]

1.1.2. Metastable- Technetium and Molybdenum

Another isotope of Tc-99 worth mentioning is technetium-metastable (Tc-99m). The short-lived Tc-99m is used as an organ radioisotope or radioactive tracer in radiopharmaceuticals in nuclear medicine [25, 26]. Tc-99m decays by gamma-emission

in 6.0 hours to Tc-99g ground state, limiting radiation dose to the patient. Tc-99m is obtained from the decay product of Mo-99, as illustrated in the flow chart below:

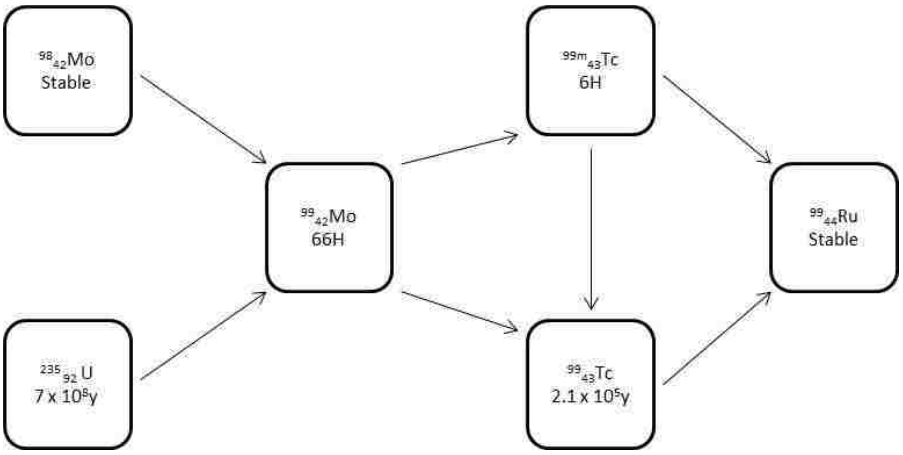

Figure 1.4: Generation and Decay of Tc-99m and Tc-99g [23]

Tc-99m, is used in about two-thirds of all diagnostic medical isotope procedures in the U.S. Tc-99m is currently produced through a multistep process that begins with the neutron irradiation of fissile U-235 contained in High Enriched Uranium (HEU) or Low Enriched Uranium (LEU) targets in a nuclear reactor. The irradiation of U-235 causes fission and production of a variety of products which contain appreciable amounts of Mo-99, I-131 and Xe-133. These fission products are obtained in the same proportions independent of whether HEU or LEU targets are used. Following irradiation, the targets are dissolved and chemically processed to separate Mo-99 from the other fission products. If desired, other fission products of interest for medical applications such as Xe-133 and I-131 could be recovered separately as well. A solution containing the

separated Mo-99 is passed through an alumina (Al_2O_3) column with the majority of the Mo-99 adsorbed on the column. The process is not efficient with approximately 30% of molybdenum being lost during the process. The columns are then shipped to hospitals in radiation-shielded cartridges for use as technetium generators [4, 27].

The Mo-99 contained in the generators, decays with about a 66 hour half-life to Tc-99m. Tc-99m is typically recovered by passing a saline solution through the alumina column in the generator, a process known as eluting the generator. The saline removes the Tc-99m daughter, but leaves the Mo-99 mother in place [27].

In 2006 the demand for Mo-99 in the U.S. ranged from 5,000 and 7,000 6-day curies per week. The demand for Mo-99/Tc-99m in the U.S. is projected to grow between 1 to 5 percent over the next 5 years, however based on the current use will likely continue to grow at a rate of 3 to 5 percent per year [27]. The problem arose because of miscalculation of challenges building nuclear reactors.

There are preexisting technologies being tested to target the manufacturing of Mo-99 from Mo-98 by neutron capture instead of solely from U-235 fission, but there are many concerns with this method of synthesis [26, 27]. The electrochemical methods developed in this thesis may be used to potentially recover and separate then purify Mo-99 to obtain Tc-99m.The basis of this application is that Tc-99m which only emits γ-rays and decays to Tc-99 in 6.01 hours limiting the overall radioactive dosage in the patient [23]. In addition, ligand functionalization of Tc-99m is possible and there are at least 31 commonly used radiopharmaceuticals that have been developed for imaging and functional studies of the brain, myocardium, thyroid, lungs, liver, gallbladder, kidneys, skeleton, blood and tumors [23].

The impending Mo-99 shortage has physicians exploring innovative and restoring old techniques; for example thallium imaging and the use of software and endoscopic cameras. However, there is a risk of decreasing accuracy which may occur because of a lower the dose of Tc-99m that can lead to false negatives and positives. Alternative thallium protocols are being investigated for replacement yet it would be used a preliminary imaging test which would be coupled with Tc-99m if the results were not conclusive. When using Tc-99m a lesion of 3mm can be detected.

1.2 Perrhenate and Pertechnetate Analogues

For many years most of the chemistry of Tc complexes was predicted on the basis of the knowledge of Re analogues. Now Tc chemistry is better known and in many cases the behavior of Re radiopharmaceuticals is predicted taking into account the reactivity of Tc labeled molecules. However, obtaining working quantities of Tc-99 is challenging based on the ability to reclaim these materials from extraction. However, perrhenate (ReO_4^-) is an analogous material that can be utilized to approximate the properties of TcO_4^-. In addition, the perrhenate can be used as an equivalent model for Tc under identical solution parameters encountered for processing used nuclear fuel. For example, the oxidation/reduction of ReO_4^- in an aqueous solution has been studied at platinum and gold working electrodes. These studies have yielded useful electrochemical potential data that is summarized in the following Table for the electrodeposition of rhenium species from aqueous solution:

Table 1.1: Electrochemical deposition of Rhenium species from Perrhenate Solutions at Platinum and Gold working electrodes [28]

	Electrodeposited species	Method used to determine oxidation state
Pt	ReO_2	Voltammetric charge calculations
Pt	ReO_2	Voltammetric charge calculations
Pt	ReO_2	Kinetic studies
Pt, Au	ReOx	Radiometric and voltammetric calculations
Pt	ReO_2, ReO_3, Re_2O_5	Comparison of voltammetric behavior with pure oxides
Au	Re	SEM-EDS*
Pt	ReO_3	SEM-EDS
Au	Re	SEM-EDS

*SEM-EDS- Scanning Electron Microscope-Energy Dispersive X-ray Spectroscopy

At neutral pH solutions Tc complexes are slightly more unstable than those of Re, decomposing to TcO_4^- and TcO_2. In acidic pH, where $[MO(OH)L_2]^{2+}$ cations are predominant, the stability of Re complexes does not change, while Tc complexes decompose very quickly. A redox process is involved in this decomposition, making TcO_4^- and TcO_2 final products. Differences in reactivity may be due to either kinetic or thermodynamic factors. With all complexes having central atoms in the same oxidation state, a dominant thermodynamic effect is highly probable. Where relative rates of electron transfer to and from analogous Tc and Re complexes are likely to be governed primarily by differences in redox potentials [29].

The main objective of the research presented in this thesis is to:

1- Evaluate the aqueous parameters for rhenium and molybdenum electrochemistry, specifically pH, solution matrix and potential window.
2- Electrochemically reduction Re(VII) to Re(0) in room temperature ionic liquid as an analogue for technetium recovery
3- Investigate electrochemical behavior of Mo(VI) and Mo(IV) in aqueous and non-aqueous environments for targeted Mo metal deposition.

Chapter 2

Electrochemical Methods

2.1 Background and Motivation

Electrochemistry is the branch of chemistry concerned with the oxidation/reduction of chemical species and the corresponding rate of electron transfer. A large part of this field deals with the study of chemical changes caused by the passage of an electric current and the production of electrical energy through controlled chemical reactions. The field of electrochemistry encompasses a huge array of different phenomena (electrophoresis and corrosion), devices (electrochromic displays, electroanalytical sensors, batteries, and fuel cells), and technologies (electroplating of metals and the large-scale production of aluminum and chlorine). In addition, the reclamation of select chemical species from aqueous or non-aqueous solutions using electrochemical methods is an attractive method because it is clean, efficient, and inexpensive relative to other methods including extraction, sorption, and refining [30].

2.1.1 Overview of electrode processes

Electrochemical systems are concerned with the processes and factors that affect the transport of charge across the interface between two distinct chemical species or phases. For our studies the interactions are defined based on a stationary electronic conductor (an electrode) and a chemical species within an electrolyte matrix. The electrode interface is critical and it directly influences charge transport and electron transfer between the chemical species and electrode surface.

Electrode materials include solid metals (Pt, Au…), liquid metals (Hg, amalgams), carbon (graphite), and semiconductors (indium tin oxide, Si). In the aqueous/non-

aqueous phase, the solution conductivity is influenced by the concentration of the supporting electrolyte or inherent concentrations of ions. The most frequently used electrolytes are liquid solutions containing ionic species (e.g.: H^+, Na^+, Cl^-) in either water or aqueous/non-aqueous solvents. To be useful in an electrochemical cell the solvent/electrolyte system must have sufficiently low resistance for electrochemical response to be observed. Less conventional electrolytes including fused salts (e.g.: molten NaCl-KCl eutectic, room temperature ionic liquids) and ionic conductive polymers (e.g.: Nafion) rely on the inherent ionic conductivity in charge transfer reactions [30].

Electrochemistry does not occur at a single interface, because most experiments do not occur within such an isolated boundary. Instead, there is set of interfaces called electrochemical cells and these systems are defined generally as two electrodes separated by a least one electrolyte phase. The difference in electric potential is typically measured between the electrodes in an electrochemical cell with a high impedance voltmeter or potentiostat. The cell potential, is measured in volts (V), where 1 V = I joule/coulomb (J/C), is a measure of the energy available to drive charge externally between the electrodes. It is a collection of the measured differences in electric potential between all of the various phases in the cell. The transition in electric potential in crossing from one conducting phase to another usually occurs almost entirely at the interface. The sharpness of the transition implies that a very high electric field exists at the interface, and it is expected to exert those effects on the behavior of charge carriers (electrons or ions) in the interfacial regions. Also the magnitude of the potential difference at an interface affects the relative energies of the carriers in the two phases; it controls the

direction and rate of charge transfer. Therefore the measurement and control of cell potential is one of the most important aspects of electrochemistry and the driving force for controlled electrochemical reactions.

The overall chemical reaction that takes place in a cell is made up of two independent half-cell reactions which describe the real chemical changes that are occurring at the two electrodes (working and counter electrodes). Each half-reaction responds to the interfacial potential difference at the corresponding electrode because the chemical composition of the system near the electrodes is different. Usually only one reaction is of interest and the electrode at which it occurs is called the working electrode. In our electrochemical system of interest the following reactions were of interest:

Table 2.1: Redox Couples, Half Reaction, and Standard Potentials for the Possible Reactions Occurring in Solution for Rhenium [31]

Redox Couple	Half Reaction	E^o (V)
$\boldsymbol{ReO_4^-/Re}$	$ReO_4^- + 8H^+ + 7e^- \rightarrow Re + 4H_2O$	0.34
$\boldsymbol{ReO_4^-/ReO_2}$	$ReO_4^- + 4H^+ + 3e^- \rightarrow ReO_2 + 2H_2O$	0.51
$\boldsymbol{ReO_2/Re}$	$ReO_2 + 4H^+ + 4e^- \rightarrow Re + 2H_2O$	0.252
$\boldsymbol{ReO_4^-/Re^{3+}}$	$ReO_4^- + 8H^+ + 4e^- \rightarrow Re^{3+} + 4H_2O$	0.422
$\boldsymbol{ReO_2/Re^{3+}}$	$ReO_2 + 4H^+ + e^- \rightarrow Re^{3+} + 2H_2O$	0.2
$\boldsymbol{Re^{3+}/Re}$	$Re^{3+} + 3e^- \rightarrow Re$	0.3
$\boldsymbol{H^+/H_2}$	$2H^+ + 2e^- \rightarrow H_2$	0.0-0.05
$\boldsymbol{H^+/H_{ad}}$	$H^+ + e^- \rightarrow H_{ad}$	0.05-0.38
$\boldsymbol{NO_3^-/NO_2^-}$	$NO_3^- + H_2O + 2e^- \rightarrow NO_2^- + 2OH^-$	0.01

Table2.2 Redox Couples, Half Reaction, and Standard Potentials for the possible Reaction Occurring in Solution for Molybdenum [31]

Redox Couple	Half Reaction	$E^0(V)$
MoO_2/Mo^{3+}	$MoO_2 + 2H^+ + e^- \rightarrow Mo^{3+} + 2H_2O$	-0.008
MoO_4^{2-}/MoO_2	$4H^+ + MoO_4^{2-} + 4e^- \rightarrow MoO_2 + 2H_2O$	n/a
MoO_2/Mo	$MoO_2 + 4H^+ + 4e^- \rightarrow Mo + 2H_2O$	-0.152
Mo^{3+}/Mo	$Mo^{3+} + 3e^- \rightarrow Mo$	-0.2

Therefore to focus on the reaction at a single working electrode a reference electrode was used to standardize the other half cell. This electrode is made up of phases having essentially constant composition and potential. The normal hydrogen electrode (NHE) is the historical reference that is used in literature but is not very convenient experimentally. Similarly the saturated calomel electrode (SCE) which uses $Hg/Hg_2Cl_2/KCl$ (saturated in water) is not commonly used due to the environmental concerns regarding mercury. For all aqueous measurements performed the silver-silver chloride electrode, Ag/AgCl/KCl (saturated in water) was used.

The fixed potential at the reference electrode is predicated on the composition of the electrode not changing as reactions take place at the working electrode. A third electrode, a Pt counter electrode is used to ensure that the potential of the reference electrode does not change as reactions occur at the working electrode. The counter electrode acts as an electron donator and acceptor during the electrochemical reaction without changing the composition of the reference. Therefore, the potential of the working electrode can poised versus the reference electrode influencing the energy of the electrons and reactivity at the electrode surface. Oxidation/reduction at the working electrode occurs as the energy of the working electrode is raised or lowered as a function

of the applied potential. When the energy of the working electrode is sufficiently negative of the reduction potential of the chemical species is reduced. When the energy of the working electrode is sufficiently positive of the oxidation potential of the chemical species, the species is oxidized. The critical potentials at which these processes occur are related to the standard potential, E^o, of the chemical species in solution.

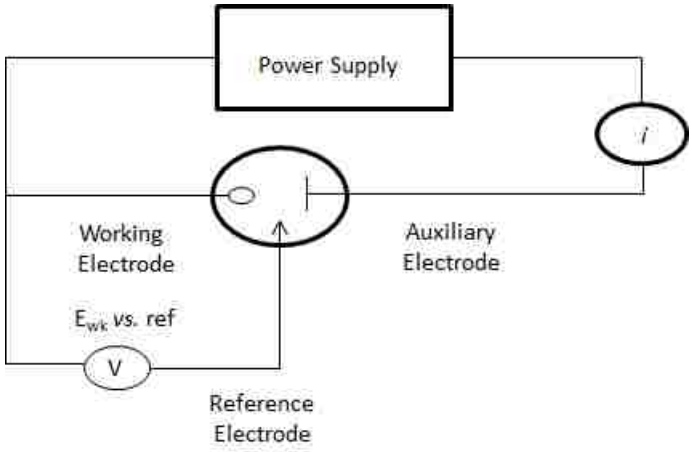

Figure2.1: Schematic Diagram of the Electrochemical Cell [30]

When considering the overall electrode, reaction: $O + ne \leftrightarrow R$ defines the conversion of the dissolved oxidized species, O, to a reduced form R, the electrode reaction rate is typically governed by the following:

1. Mass transfer (e.g.: of O from the bulk solution to the electrode surface).
2. Electron transfer at the electrode surface
3. Chemical reactions preceding or following the electron transfer, which might be homogeneous processes or heterogeneous ones on the electrode surface.

4. Other surface reactions, such as adsorption, desorption, or crystallization.

The rate constants for some of these processes (e.g.: electron transfer at the electrode surface or adsorption) are dependent upon the applied potential [30].

The simplest reactions involve only mass transfer of a reactant to the electrode, heterogeneous electron transfer involving non-adsorbed species and mass transfer of the product to the bulk solution. In our case the bulk solutions for our system used H^+ and RTIL as electrolyte. More complex reaction sequences involving a series of electron transfers and protonation, branching mechanisms, parallel paths, or modifications of the electrode surface are quite common. For our systems, this is the path that is predicted for the electrochemical reduction of the Re/Mo species. When a steady-state current is obtained the rates of all reactions steps in a series are the same. The rate determining step determines the extent the current is limited by the inherent inhibition of one or more reactions. More thermodynamically favorable reactions have reduced rates due to kinetic limitations associated with the rate-determining step.

2.2 Cyclic Voltammetry Technique

Basic electrochemical behavior of a system can be obtained through a series of steps to different potentials and recording the current-time curves. While potential step methods are useful, more information can be gathered by sweeping the potential as a function of time while recording the current. The potential is usually varied linearly with time at sweep rates (ν) ranging from 10mV/s to 1000mV/s with conventional electrodes. When the potential is scanned in only "on" direction and the current is measured, the technique is referred to as linear potential sweep chronoamperometry, or more commonly as linear sweep voltammetry (LSV) [30]. Cyclic voltammetry implies that both the

forward and reverse potential scans are conducted and the current is measured. The technique allows both oxidation and reduction processes to be measured for the system because the polarization of the electrode is reversed on the reverse scan [30]. This approach is designed to provide a direct observation of a reduced species after the more oxidized state is generated in solution. This is useful for evaluating the reduced species participation in chemical reactions on electrochemical time scales [30].

2.3 Underpotential deposition

Bulk electrolysis techniques can be classified by a controlled parameter (E or i) and by the quantities actually measured or by the process carried out. In controlled-potential techniques the potential of the working electrode is maintained above the standard potential for a given chemical reaction and continued over the course of the process. The driving force for the chemical reaction is the applied potential at the working electrode which controls the rate of the electrolytic process. The technique is the preferred method for bulk electrolysis. The method requires potentiostats with large output current and voltage capabilities and the need of a stable reference electrode, carefully placed in proximity to the working electrode to minimize uncompensated resistance. Placement of the auxiliary electrode is also important to provide a uniform current distribution across the surface of the working electrode [30].

In controlled current techniques, the current passing through the cell is held constant and programmed to change with time. These techniques involve simpler instrumentation however they do require either a special set of chemical conditions in the cell or specific detection methods to signal completion of the electrolysis and to ensure current efficiency. Measures need to be taken to ensure that the electrode potential does not

move into a region where undesirable side reactions will occur (i.e. H_2(g) evolution, water oxidation, and metal oxidation) [30]. Therefore, any electrochemical reaction is bound by hydrogen evolution at negative potentials and water oxidation at positive potentials, limiting the potential window that can be utilized.

2.5 Quartz Crystal Microbalance

In many electrochemical experiments, mass changes occur as material is either deposited on or lost from the electrode. The reduction process results in deposition, while oxidation initiates dissolution. Cyclic voltammetry can be used to evaluate the surface processes but is often convoluted by solution based oxidation/reduction processes. Electrochemical quartz crystal microbalance (EQCM) is a method that allows surface and solution processes to discern these changes simultaneously. The quartz crystal has a resonance frequency of oscillation that can be used to measure the mass deposited at an electrode on the surface of the material. The bare quartz crystal resonant mode depends upon its size thickness and oscillates at a frequency, f_0. The frequency of oscillation is sensitive to mass changes on the crystal surface as expressed by the Sauerbrey equation:

$$\Delta f = -\frac{2f^2 mn}{(\rho\mu)^{1/2}} = -C_f m$$

whereΔf is the frequency change caused by addition of a mass per unit area, m, to the crystal surface, n is the harmonic number of the oscillation, μ is the shear modulus of quartz, and ρ is the density of quartz. The constants are usually lumped together to yield a single constant, the sensitivity factor, C_f. However the behavior depends on the medium in which the crystal is operating, because the medium couples (or "loads") to the crystal surface and the affects the shear mode. Thus, f_0 and C_f values in liquids are lower

than those in air or vacuum. The frequency of oscillation is also a function of temperature. The density and viscosity of a solution in which the crystal is operating can also affect the frequency [30]. When external stimuli are minimized the frequency change is proportional to the mass deposited which can be related to the charge passed from the voltammetric response.

2.4.1 Electrochemical Quartz Crystal Microbalance Apparatus

A schematic diagram of the apparatus for QCM in an electrochemical experiment is given below in Figure 2.2.

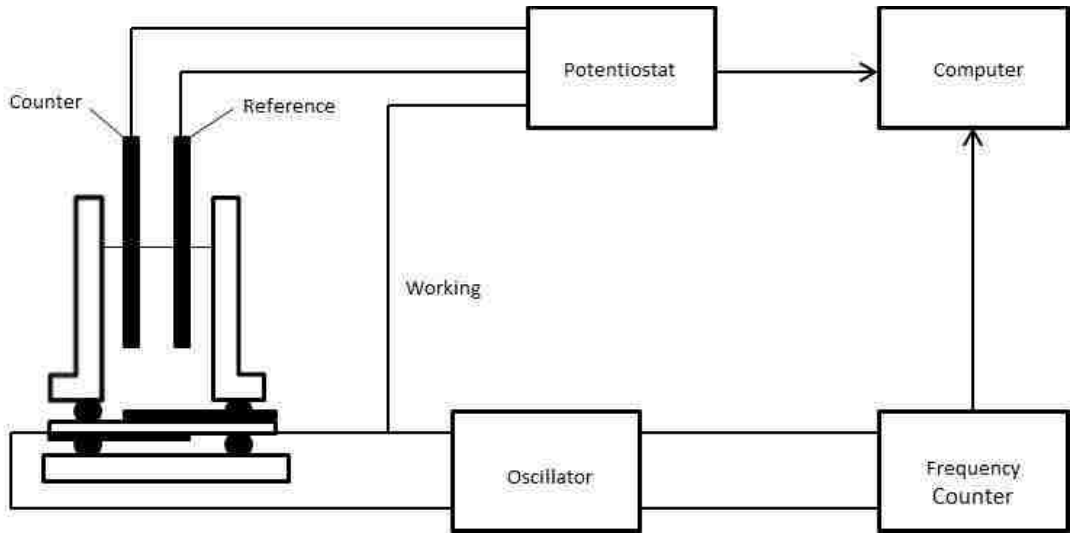

Figure2.2: Schematic Diagram of Cell and Apparatus for Electrochemical QCM Studies

The quartz crystal is frequently clamped in an appropriate O-ring joint to expose only one of the contacts to the solution. This contact (usually Au or Pt) is also the working electrode and is part of both the potentiostats and oscillator circuits. The crystal is driven

by a broadband oscillator circuit that tracks the resonant frequency of a crystal, measured with a commercial frequency counter, during electrochemically-induced mass changes on the electrode surface.

The QCM has been used in many types of electrochemical studies involving mass changes on electrodes, including the underpotential deposition of metals, adsorption/desorption [30].

2.5 Scanning Electron Microscope

The Scanning Electron Microscope (SEM) is a non-contact microscopy technique that scans the surface of a sample with a narrow, highly-collimated beam of high-energy electrons. The electron interaction with the atoms that make up the sample produce signals that contain information about the sample's surface, composition, and other properties such as electrical conductivity. The types of interactions between this beam and the sample's surface cause secondary electrons due to inelastic scattering, which are then detected by an electron detector. This technique is sometimes referred to as Secondary Electron Microscopy because of the secondary electron emission mechanism [32, 33].

2.5.1 Energy-dispersive X-ray Spectroscopy (EDS)

EDS is an analytical technique used for the elemental analysis or chemical characterization of a sample. It relies on the investigation of a sample through interactions between electromagnetic radiation and matter, and the analyzing X-rays emitted by the matter in response to being hit with charged particles. Its characterization capabilities are due in large part to the fundamental principle that each element has a unique atomic structure allowing the x-rays that are characteristic of an element's atomic

structure to be identified uniquely from one another. To stimulate the emission of characteristic x-rays from a specimen, a high-energy beam of charged particles (electrons) is focused into the sample being studied. At rest, an atom within the sample contains ground state electrons in discrete energy levels bound to the nucleus. The incident beam excites an electron in an inner shell, ejecting it from the shell while creating an electron where the electron was. An electron from an outer, higher-energy shell then fills the hold, and the difference in energy between the higher-energy shell and the lower energy shell are released in the form of an x-ray. The number and energy of the x-rays emitted from a specimen can be measured by an energy-dispersive spectrometer. The energy of the x-rays are characteristic of the difference in energy between the two shells, and of the atomic structure of the element, from which they were emitted, allowing the elemental composition of the specimen to be measured [32, 34].

The experimental and instrumental techniques described will be utilized to analyze the electrochemical reduction of Rhenium and Molybdenum in aqueous and non-aqueous systems.

CHAPTER 3

CHARACTERIZATION OF ELECTROCHEMICAL AND AQUEOUS SOLUTION PARAMETERS

3.1 INTRODUCTION/ MOTIVATION

Rhenium has been used in the experiments presented in this chapter to model the properties of technetium due to its scarcity and radioactivity. Rhenium and technetium behave as analogous materials under similar chemical conditions which allow us to model the properties of technetium using a material that is easy to obtain with no radioactivity [29]. The experiments with rhenium are performed using solution conditions that mimic those for technetium obtained from used nuclear fuel processes (dissolved in a 1.0 - 3.0 M HNO_3 solution) to ensure that the electrochemistry experimentation with rhenium are consistent with those that would be used for comparable technetium experiments. It is also important to discuss molybdenum which is relevant because it is directly linked to the derivation of Tc-99m; the radioactive isotope is predominantly used for medical imaging applications.

Evaluating the oxidation/reduction properties of perrhenate, and molybdenum is important because recovering the target species from aqueous solutions as metals or metal oxides may be possible using electrochemical methods. Previous studies have examined the influence of acidity and pH on the electrochemical deposition of Re at Pt and Au surfaces from solution containing perrhenate [28, 35, 36]. In this chapter we explore the electrochemistry of Re and Mo in protic aqueous solution expanding on previous work to include pH dependence, supporting electrolyte solution composition, and the electrode composition in the recovery of rhenium and molybdenum.

3.2. Re Electrochemistry: pH and solution composition at Pt and Au surface.

The pH of aqueous systems plays an integral role in the electrodeposition of any rhenium species from a ReO_4^- solution [37]. Although the pH is a critical parameter in Re deposition, the solution conditions and composition have not been extensively studied or articulated in literature. For example, one study demonstrates that pH plays an essential part in the electrodeposition of ReO_4^-[28]. However, Re oxide was the final product where the end goal was the deposition of Re metal [28, 38]. Our experiments further examine the dependence of pH and solution conditions that are suitable for Re *metal* deposition from a perrhenate solution.

The electrochemistry of ReO_4^- was examined in solutions containing high acidity (low pH). For example, an initial solution contained 4.0 mL of an aqueous solution containing 89 mM ReO_4^-. The pH of the solution was adjusted through the addition of 500 µL of 1.0 M HNO_3 aliquots with the initial pH of 0.30 was lowered to a final pH of 0.02. Cyclic voltammetry (CV) measurements were obtained after each addition of HNO_3 in the potential range of 1.0 V to 0.0 V vs. Ag/AgCl reference electrode with a Pt working electrode. Electrochemical activity for Re was not observed regardless of the scan rate or potential range utilized for these preliminary studies. It is difficult to conclude whether these results are consistent with previous finding because the previous measurements utilized other acids that may have influenced the electrochemical processes (i.e.: $HClO_4$, H_2SO_4) [28]. Moreover, the electrochemical reduction of ReO_4^- may not occur in solution because the species required for reduction were not present at the pH values utilized (i.e.: ReO_2, Re^{3+}) [28].

The pH of the aqueous solution was increased to determine if the deposition of Re could be observed under less acidic conditions, Figure 3.1(a). A change in the initial solution was made by dissolving the ReO_4^- in 1.0 M HNO_3 instead of H_2O. That initial solution contained 89 mM ReO_4^- dissolved in 1.0 M HNO_3 (with a pH of 0.17). The electrochemical response was obtained for this solution and after sequential additions of 100 µL aliquots of 1.0 M NaOH with the pH = 0.34 after 200 µL of 1.0 M NaOH was added. Significant electrochemical activity was observed at this pH as shown from Figure 3.1(b). Finally, the electrochemical response was again significantly diminished after the addition of an additional 200 µL of NaOH (increasing the pH to 0.41), Figure3.1(c).

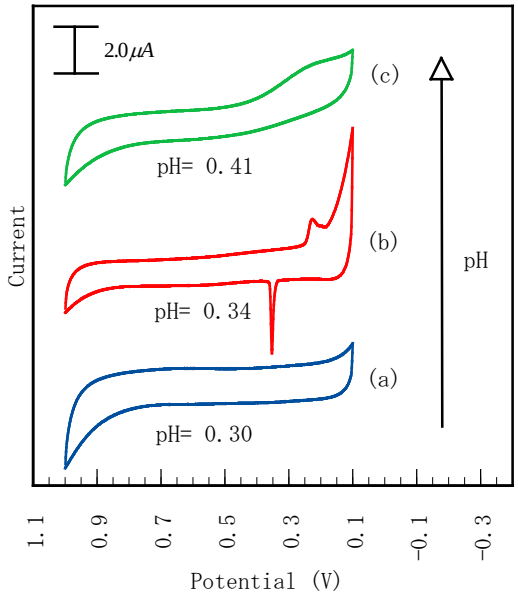

Figure 3.1: Cyclic Voltammetric Response of a Pt Electrode as a Function of pH in a Solution Containing 0.089 M ReO_4^-

It is evident that the pH range is extremely narrow, providing a limited thermodynamically stable electrochemical window for Re deposition. The narrow pH range associated with the deposition of Re demonstrates the importance of pH on the reduction of Re(VII) to Re(0) in aqueous solution. The possible reactions that govern the reduction process are provided below:

$$ReO_4^- + 8H^+ + 7e^- \rightarrow Re + 4H_2O$$

$$ReO_4^- + 4H^+ + 3e^- \rightarrow ReO_2 + 2H_2O$$

$$ReO_2 + 4H^+ + 4e^- \rightarrow Re + 2H_2O$$

The relevant half-cell reactions in aqueous solution are presented in Table 3.1:

Table 3.1: Redox Couples, Half Reaction, and Standard Potentials for the Possible Reactions Occurring in Solution[31]

Redox Couple	Half Reaction	E^o (V)
ReO_4^-/Re	$ReO_4^- + 8H^+ + 7e^- \rightarrow Re + 4H_2O$	0.34
ReO_4^-/ReO_2	$ReO_4^- + 4H^+ + 3e^- \rightarrow ReO_2 + 2H_2O$	0.51
ReO_2/Re	$ReO_2 + 4H^+ + 4e^- \rightarrow Re + 2H_2O$	0.252
ReO_4^-/Re^{3+}	$ReO_4^- + 8H^+ + 4e^- \rightarrow Re^{3+} + 4H_2O$	0.422
ReO_2/Re^{3+}	$ReO_2 + 4H^+ + e^- \rightarrow Re^{3+} + 2H_2O$	0.2
Re^{3+}/Re	$Re^{3+} + 3e^- \rightarrow Re$	0.3
H^+/H_2	$2H^+ + 2e^- \rightarrow H_2$	0.0-0.05
H^+/H_{ad}	$H^+ + e^- \rightarrow H_{ad}$	0.05-0.38
NO_3^-/NO_2^-	$NO_3^- + H_2O + 2e^- \rightarrow NO_2^- + 2OH^-$	0.01

The reactions suggest, that the solution composition and mole ratios of the Re species may be critical in determining the feasibility of reducing the initial speciesReO_4^- to Re metal in aqueous solutions. In addition, the reactions suggest the role of proton in the reduction processes cannot be neglected.

It has been postulated that reduction of ReO_4^- is aided by adsorption of H_{ad} at the surface of the electrode or through the formation of ReO_2, which can function as reducing agent on the electrode surface [28]. The reduction of ReO_4^- is strongly influenced by proton adsorption at the surface because in an aprotic medium, such as acetonitrile, no reduction current was observed, even at potentials as negative as - 2.2 V; with typical reduction potentials of ~ 0.2 V. The nature of the reducing agent in the electrochemical reduction of ReO_4^- is an important factor with proton adsorption at the electrode surface playing a critical role. For example, ReO_4^- reduction can be accomplished through direct electron transfer from the electrode or with the participation of H_{ad}. The reduction of $ReO_4^-$is not achieved in aprotic medium suggesting that H_{ad} acts as reducing agent for ReO_4^- on the Pt surface. In addition, H_{ad} also participates in the formation of sub-monolayer quantities of ReO_2. Therefore the solution pH and composition are important because of the species that needs to be present in order for the reduction of ReO_4^-.

The composition of the electrolyte in the electrochemical system is another factor important in the kinetics and the ability to deposit Re species onto working electrodes (i.e.: Pt, Au, or GC). The rate of the electrodeposition of any Re species at a given potential strongly depends on the nature of the anion(s) present in the supporting electrolyte. Rhenium was dissolved in 1.0 M HNO_3 because the solution parameters need to be similar to those in which TcO_4^- is found from used nuclear fuel. For each of

the electrodes studied, the electrochemical reduction of Re species take place at thermodynamic potentials that are close to the potentials for H_2(g)evolution and water hydrolysis with the following reactions:

$$2H^+ + 2e^- \rightarrow H_2$$

$$4H^+ + O_2 + 4e^- \leftrightarrow 2H_2O$$

The H_2(g) evolution occurring at potentials lower than 0.0 V and water oxidation at more positive potentials. Therefore, surface pH changes are possible at the electrode as H_2(g) evolves or as H^+ is consumed or produced during electrolysis [31]. These side reactions can lower the bulk pH, the concentration of species at the electrodes surface, increasing the acidity in the vicinity of the electrode, influencing the rate of NO_3^- reduction and other side reactions.

$$H^+ + e^- \rightarrow H_{ad}$$

$$NO_3^- + H_2O + 2e^- \rightarrow NO_2^- + 2OH^-$$

For example, in previous studies it was found that the reduction of $HClO_4$ interfered with the reduction of ReO_4^-because the Re adsorbed layers became catalysts and reduced $ClO_4^-$to Cl^- at potentials more negative than 0.3 V [28]. The reduction of ReO_4^- became a competitive surface reaction therefore it was important to ensure that the NO_3^-/NO_2^- species did not interfere with the reduction of ReO_4^-. A background voltammogram for a Pt electrode immersed in a solution containing 1.0 M HNO_3 is compared to the voltammetric response of a Pt electrode immersed in a solution containing ReO_4^-, Figure3.2.

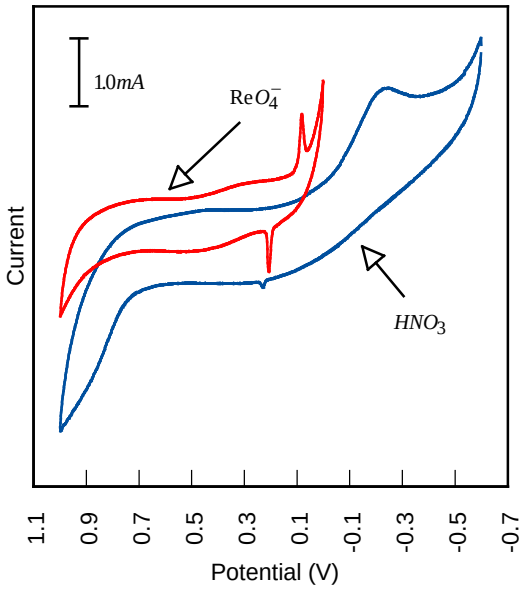

Figure3.2: Cyclic Voltammetric Response of 89 mM ReO_4^- dissolved in 1.0 M HNO_3 with 200 µL of 1.0 M NaOH on a Pt Working Electrode Compared to the Background of 1.0 M HNO_3 with Pt Working Electrode at a pH of 0.34

From Figure3.2 we can see that the reduction of HNO_3 occurs at a different potential than the Re species obtained from the perrhenate solution. In addition, the sharp reduction waves associated with the initial reduction of ReO_4^- at 0.1 V are not observed when HNO_3 is present. Although no inhibition was observed with this system, it is important to minimize any possible interferences to ensure that the deposition of Re at electrode surfaces is optimized.

In conclusion the ideal pH range and solution parameters were found which allow for the examination of Re electrochemistry at Pt and Au substrate metals. Furthermore these principles can be applied to the electrochemical reduction of Mo at Pt and Au substrates as well. The combined studies should provide information that will allow the targeted

electrochemical reduction and reclamation of Tc species derived from fission products or from the use in pharmaceutical applications.

3.3 The Electrochemistry of Rhenium at Gold and Platinum Electrodes

Electrochemical reactions that occur at platinum and gold substrates are influenced by similar solution and chemical parameters. For example, both electrodes have competing reactions (H_2 evolution and water hydrolysis) that limit the potential window which can be utilized for electrochemical measurements in aqueous solution. However, the reactions which define the potential window are influenced by electrode kinetics and do not occur at the same potentials for the Au and Pt electrodes. For example, hydrogen gas evolution at the Pt electrode occurs at potentials more **negative** than 0.0 V which inhibits the electrochemical reduction occurring at the surface. Hydrogen evolution is more prominent at the Pt electrode with measureable current at potentials negative of 0.0 V, under the same conditions $H_2(g)$ is not observed at the Au working electrode. The evolution of $H_2(g)$ disrupts the electrochemical reduction of the target species, however the H_{ad} aides in the reduction. The difference in potentials for the Pt working electrode is ~ 0.05 V which is very narrow potential window and the reduction of Re is minimized due to the competing reaction. Below in Figure 3.3, is a schematic of what occurs at the Pt electrode surface with H_{ad} versus $H_2(g)$:

Figure 3.3: Schematic of the H_{ad} vs. H_2(g) Evolution Occurring at the Pt Working Electrode

The potential window for Au is slightly larger, with H_2 evolution occurring at potentials negative of – 0.3 V. Ideally, the potentials windows for Pt and Au are 1.0 V – 0.0 V and 1.0 V - -0.1V, respectively. The solution to measure ideal potential windows for each metal (Pt, Au) is at their optimal solution parameters (pH 0.34). To illustrate the importance of potential windows, Au and Pt were both run at the potential window for Au. Figure 3.4 shows the H_2(g) evolution while none occurs at the Au electrode.

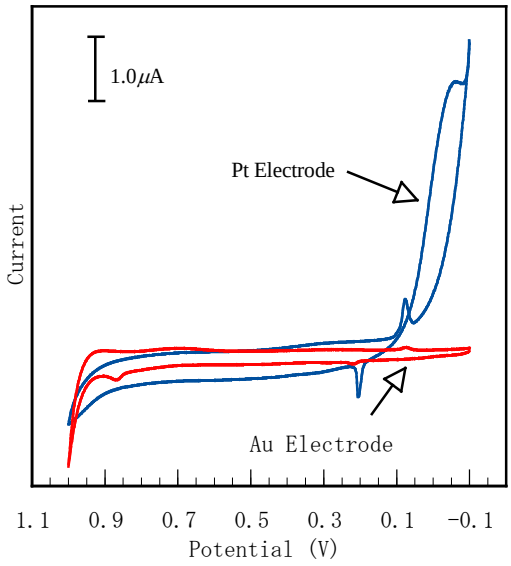

Figure 3.4: Cyclic Voltammetric Response of 89 mM ReO_4^- Dissolved in 1.0 M HNO_3 Analyte Solution at Target pH of 0.34: Comparing the Potential Window of Platinum and Gold Working Electrodes

The potential window for Pt and Au in these solution conditions is 1.0 V to 0.0 V and 1.0 V to -0.1 V, respectively. The potential window for platinum is purposely wide to illustrate the historesis associated with hydrogen evolution ~0.0 V, which can be seen in Figure 3.4. The electrochemical limitations for Au and Pt metals in aqueous solution are primarily based on hydrogen evolution at reducing potentials.

$$2H^+ + 2e^- \rightarrow H_2$$

If the reduction process is studied under identical solution and electrochemical conditions the reduction processes for Pt and Au electrodes are very different, Figure 3.5. Reduce reduction of ReO_4^- is observed at Au because the adsorption of H^+ is diminished relative to the Pt electrode surface.

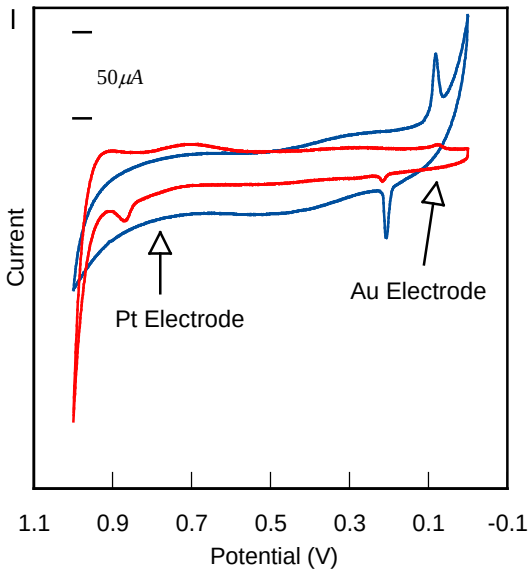

Figure 3.5: Cyclic Voltammetric Response in 3.f0 mL of M HNO_3, 2.5 mL of 0.089 M ReO_4^-, and 200 µL of 1.0 M NaOH at a Scan rate of 10mV/s

Therefore, proton sorption at the Pt electrode is enhanced relative to Au and the contribution from the surface adsorption of this species in the reduction processes associated with Re cannot be neglected [28]. Optimization of ReO_4^- reduction at each substrate metal is required to optimize the processes relative to the working electrode utilized. With these parameters defined, experiments can be run based on the potential window, pH and solution conditions that optimize recovery at a given electrochemical interface in aqueous solution

3.3.1 Electrochemistry of Rhenium on Platinum Working Electrode

A more in depth analysis of Re electrochemistry was warranted after identifying the solution parameters that resolve the electrochemical deposition of rhenium at Pt surface. In Figure 3.6, is the electrochemical reduction of ReO_4^- in ideal solution conditions on a

Pt working electrode are presented based on solution parameters defined in the previous section.

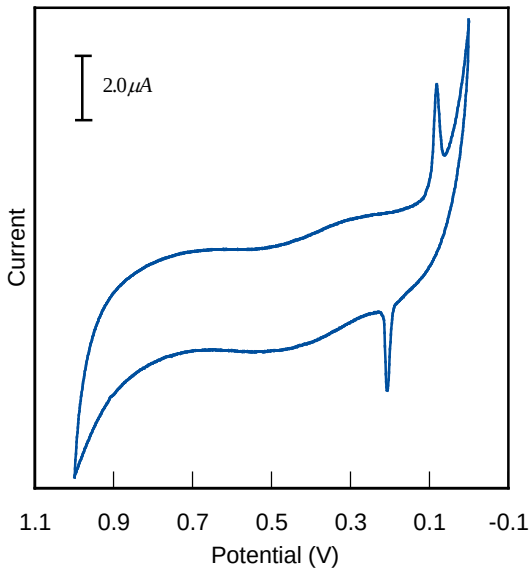

Figure3.6: Cyclic Voltammetry of a Platinum Working Electrode Immersed in a Solution Containing 3.0 mL of 1.0 M HNO_3Mixed with 2.5 mL of 0.089 M ReO_4^-Titrated to a pH of 0.34 with 1.0 M NaOH.

Previously researchers have postulated that a two-step reduction mechanism for ReO_4^- results in the deposition of Re metal at the Pt working electrode, with the adsorption occurring at the broad peak at potentials 0.4 V – 0.15 V [28]. The process involves the formation of an intermediate species, or a submonolayer of ReO_2 which is the peak ~ 0.1 V. The ReO_2 deposited on the surface acts as a reducing agent in the assisted reduction of various Re oxide species at the electrode surface (ReO_3, Re_2O_5, etc…) to produce metallic Re which corresponds to the second reduction peak at 0.05 V. The following general reduction mechanism has been proposed:

$$ReO_4^- \xrightarrow{E_1} ReOx_{ad} \xrightarrow{E_2} Re$$

The concentration of the oxides and metallic Re is dependent on the driving force associated with the applied potentials E_1 and E_2 as shown in the above mechanism and the corresponding reaction rates which are influenced by the kinetics of the reduction processes[28]. Specifically, rhenium oxides are deposited at potentials lower than 0.20 V on platinum electrodes, while reduction to metallic rhenium occurs at potentials lower than 0.10 V with the adsorption of H^+ at the electrode surface (H_{ad}).

The electrochemistry occuring at Pt electrodes can be evaluated further to determine if the voltammetry is based on surface or solution process. The previous mechanism suggests that the process is dependent on the surface adsorption of Re species followed by the reduction of these species to metal. The scan rate dependence of the peak currents can be utilized to distinguish surface and solution based processes. Specifically for solution based process a plot of the square root of scan rate ($v^{1/2}$) versus peak current (i_p) will produce a linear response indicating that solution diffusion is key. In contrast if the peak current is proportional to the scan rate it is surface process, in which H_{ad} is adsorbed. The corresponding equations for peak current are provided below for diffusion related process:

$$i_p = 0.446\left(\frac{F^3}{RT}\right)^{1/2} n^{3/2} A D_o^{1/2} C_o^* v^{1/2}$$

At 25°C, for A is the area of the electrode surface (cm^2), D_o is diffusion coefficient (cm^2/s), C_o^* is the bulk concentration (mol/cm^3), and v is the scan rate in V/s, $i_p$in amperes is:

$$i_p = (2.69 \times 10^5) n^{3/2} A D_o^{1/2} C_o^* v^{1/2}$$

These reactions are for reversible electron transfers and are useful for analyzing electrochemical reversible systems [30]. Deviations from linearity are indicative of either complications with the kinetics of the observed electron transfer or the result of chemical changes which occur as a result of the electron transfer. In our case the deviation occurs from the chemical change occuring at the surface of the electrode (i.e.: $H_{ad}/ReOx_{ad}$) which corresponds to this equation:

$$i_p = \frac{n^2F^2}{4RT}\nu A\Gamma_o^* = (9.39 \times 10^5)n^2\nu A\Gamma_o^*$$

n is the number of electrons transferred, $A\Gamma_O^*$is the moles of adsorbed O on the electrode surface; this is where the peak current (i_p) is proportional to ν, in contrast to the $\nu^{1/2}$ dependence shown for the current responses for diffusing species[30]. The electrochemical reduction of Re species at Pt surfaces was examined as a function of scan rate in Figure 3.7. The peaks in the anodic response showed very little shift in the peak potential and the current is plotted as a funciton of scan rate in Figure 3.8. Linear regession provides a correlation of $R^2 = 0.9924$ and the linear dependence of the peak current, i_p, on the scan rate, ν, indicates the electrochemistry is governed by surface adsorption. The cathodic current was treated in same manner providing a linear response when i_p is plotted versus the scan rate, ν.

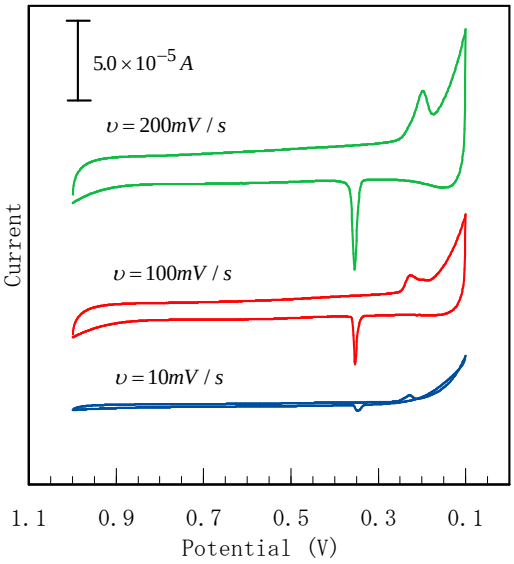

Figure 3.7: Cyclic Voltammetry Response at a Platinum Working Electrode as a Function of Scan Rate in a Solution containing 0.089 M ReO_4^- at pH of 0.34

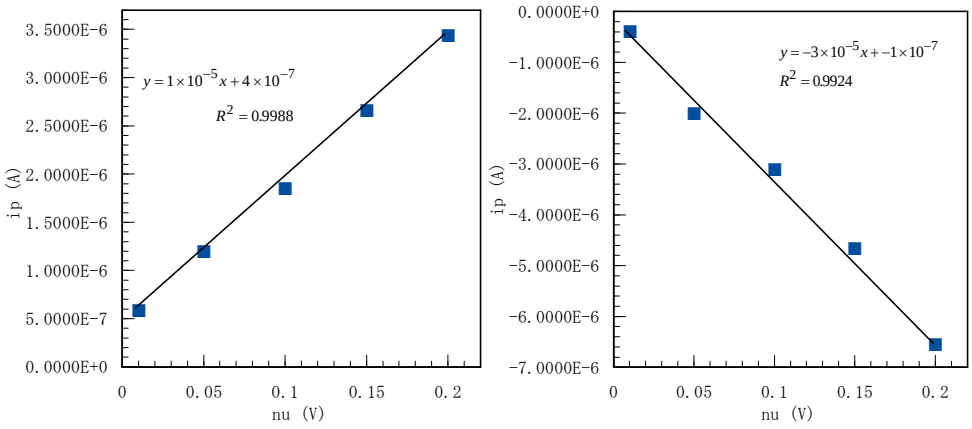

Figure 3.8: Plot of i_p vs v for the Anodic and Cathodic Current for the Cyclic Voltammetry Scans from Figure 3.7.

The plots in Figure 3.8 are indicative from the linear regression line describing that what is occurring at the surface of the Pt electrode is indeed adsorption, and that the adsorbates are interacting with each other suggesting that the sub-monolayers of

ReO_2(ad) aid in the reduction to Re metal. This can be confirmed calculating the area of the monolayer at the surface of the electrode for the peak at 0.1. V which is $4.626 \times 10^{13} \frac{atoms}{cm^2}$; which falls in the range of values for typical adsorbate coverage: $6 \times 10^{13}\ to\ \times 10^{14} \frac{atoms}{cm^2}$[30].

From these results it was deduced that H_{ad} are electrochemically formed on the electrode surface and subsequently reduce the ReO_4^- ions through a chemical reaction. The nature of the rhenium ad-layer is dependent on the adsorption potential (E_{ad}) and when E_{ad}< 0 V, metallic Re would be electrodeposited. It was also suggested that ReO_2 adsorption with a submonolayer is formed, followed by bulk phase $ReO_2 \bullet xH_2O$ that shifts towards values more positive than those corresponding to the oxidation of the ReO_2 submonolayer, due to the positive potentials at which the Pt is cycled through.

The result obtained with H-adsorbing metals (Pt vs. Au) emphasizes the participation of H_{ad} in the reduction of ReO_4^-. In this case for Pt, the initial amount of ReO_2 is formed by direct electron transfer; due to the adsorption of perrhenate on the electrode surface followed by a reduction reaction assisted through the participation of H_{ad} to yield adsorbed ReO_2. The amount of adsorbed ReO_2 depends on the surface coverage by the adsorbed perrhenate. It is important to note that the presence of H_{ad} atoms present on the electrode surface to make the following reaction feasible, which is followed by the catalytic reduction of ReO_4^- with the aid of pre-adsorbed H atoms:

$$Pt + H^+ + e^- \rightarrow Pt - H_{ad}$$

$$ReO_{4(aq)}^- + 3Pt - H_{ad} + H^+ \rightarrow Pt - ReO_2 \cdot H_2O_{ad} + H_2O$$

Once a submonolayer of $ReO_{2(ad)}$ is formed, then following redox couple is established near the electrode surface:

$$ReO_4^- + 4H^+ + 3e^- \rightarrow ReO_2 + 2H_2O$$

Although H_{ad} are needed to reduce ReO_4^-, once ReO_2 is formed the electrochemical reduction by direct electron transfer takes place at the surface based on the following reaction[28]:

$$Pt - ReO_2 \cdot H_2O_{ad} + 4e^- + 4H^+ \rightarrow Pt - Re + 3H_2O$$

3.3.2 Electrochemistry of Rhenium on Gold Working Electrode

The electrochemical behavior of aqueous ReO_4^- containing solutions on Au provides an interesting feature to be compared with Pt, due to the negligible amounts of H_{ad} atoms that can be absorbed on the surface of Au. This changes the mechanism for rhenium deposition. Below is a CV of the ReO_4^- optimal solution at a gold working electrode.

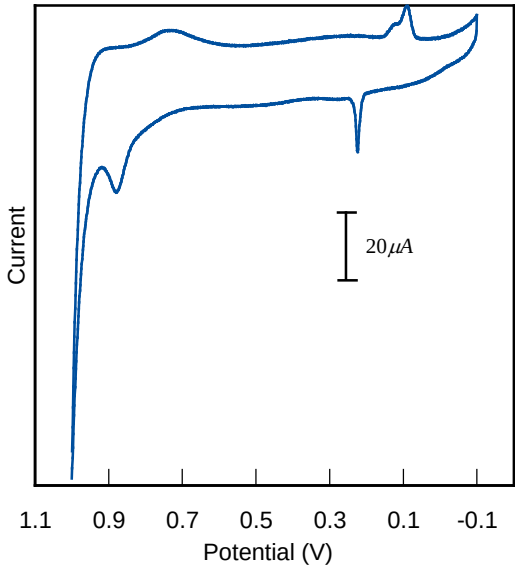

Figure 3.9: 0.089 M ReO_4^- in 1.0 M HNO_3 and 200 µL of 1.0 M NaOH on Au Working Electrode

The gold electrode has a larger potential window (-0.1 V- 1.0 V) because of the lack of H_{ad}.

The electroreduction of ReO_4^- in aqueous acid on Au takes place at potentials lower than 0.05 V, suggesting that on Au there is competitive deposition of ReO_2 and Re taking place. The extent of each process depends upon the potential and the time of adsorption. There is an initial formation of H_2(g) followed by metallic Re electrodeposition taking place. The sequence of both reduction reactions, the formation of H_2(g) followed by the electrodeposition of metallic Re, explains the presence of obstructed H_2(g) arranged between the electrodeposited Re and the Au substrate [28]. The oxidation occurs at ~0.2 V and ~0.8 V, which suggests that there is competitive deposition of both ReO_2 and Re that is taking place on the Au surface. Both processes are dependent on the chemical composition of species at the surface at a given applied potential which are:

$$ReO_4^- + 8H^+ + 7e^- \rightarrow Re + 4H_2O$$

$$ReO_4^- + 4H^+ + 3e^- \rightarrow ReO_2 + 2H_2O$$

$$ReO_2 + 4H^+ + 4e^- \rightarrow Re + 2H_2O$$

A reduction sequence has been proposed involving an adsorption of ReO_4^-, taking place at 0.6 V or downward. This process may include a partial charge transfer to the surface. At the same time, H_2(g) is evolved at E < 0.05 V according to the equation which then reduces the adsorbed perrhenate to$ReO_2 \cdot 2H_2O$,

$$Au - ReO_4 + 2H_2 \rightarrow Au - ReO_2 \cdot 2H_2O$$

then further reduced to metallic Re at $E^o = -0.50V$ according to:

$$Au - ReO_2 \cdot 2H_2O + H_2 + 2H^+ + 2e^- \rightarrow Au - Re + 4H_2O$$

The initial formation of $ReO_2 \bullet 2H_2O$ does not imply a significant increase of the Au electrode mass, while the formation of metallic Re is accompanied by the mass increase detected from the EQCM. These experiments confirm those data for which the presence of H_2 occluded in the deposit of metallic Re was established [28].

3.4. Introduction to Molybdenum

Molybdenum reduction is important because of its relevance to medical imaging and reclamation as Tc-99 in hospital waste[39]. The electrochemical reduction of molybdenum is studied in the same manner as rhenium, and targeted for molybdenum metal deposition. However, there is not much information about molybdenum redox or half-cell electrochemistry. The scheme for the reduction pathway for Mo is depicted in Figure 3.10.

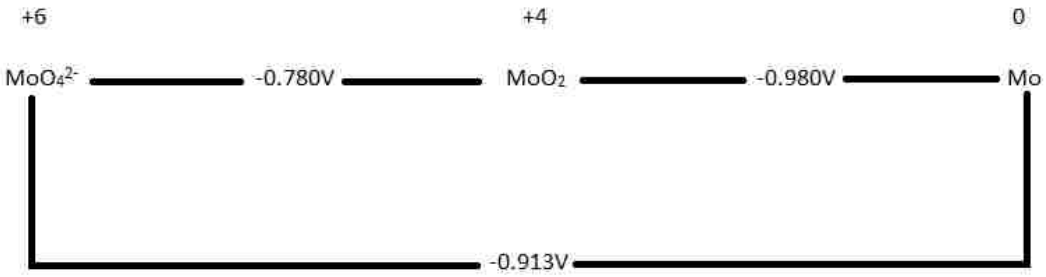

Figure 3.10: Molybdenum Oxidation State Flow Chart

It is important to note that Mo(VI) cannot be reduced below Mo(III) in an aqueous system. Under that assumption, there is an understanding that the reduction and deposition of Mo would be in the MoO_x form. The experimental parameters for Mo were

similar to the manner in which Re was treated. The same principles for optimizing the solution conditions previously discussed were applied for the Mo electrochemical reduction using Mo(IV) as MoO_2 and Mo(VI) in the form of the MoO_4^{2-}. Since the experimental conditions involve a low pH, acid hydrolysis provide additional species including $Mo_7O_{24}^{6-}$ and $Mo_8O_{26}^{4-}$ in solutions with a pH range of 6 - 1. In aqueous solutions with a pH less than 1 the following complexes may be formed: $Mo_{36}O_{112}^{8-}$, $[HMoO_3]^-$, $[H_2Mo_2O_6]^{2+}$, and $[H_3Mo_2O_6]^{3+}$[31].

3.4.1 Electrochemistry of Molybdenum

The overall reduction of the molybdenate ion occurs through a two steps mechanism where:

$$Mo(VI) \rightarrow Mo(V) \rightarrow Mo(III)$$[31]

The first experiments for the Mo series involved finding the ideal solution conditions for MoOx deposition on target substrate metals (Pt or Au). This involved adding aliquots of 100 µL of 1.0 M NaOH to a 89mM MoO_4^{2-}solution until resolved electrochemical reduction was seen, shown in Figure 3.11.

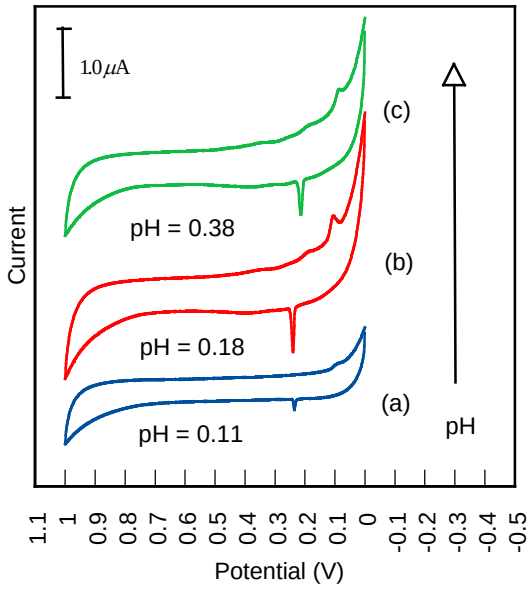

Figure 3.11: Cyclic Voltammetric Response of a Pt Working Electrode in Solutions Containing 0.01 M MoO_4^{2-} with Increasing Aliquots of 1.0 M NaOH at a Scan Rate of 100 mV/s.

The CV (Figure 3.11(a)) has 0 µL NaOH which shows a small response (pH 0.11), compared to Figure 3.11(b) which is more resolved containing 200 µL NaOH and at a pH of 0.18. In Figure 3.11(b) there is an emergence of 2 peaks that are not visible in Figure 3.11(a), increasing the base concentration facilitates the reduction of MoO_4^{2-}. The resolution of the reduction peaks is lost as more NaOH was added, Figure3.11(c).

The Mo series of experiments were optimized by dissolving them in 1.0 M HNO_3 and adjusting the pH to 0.18 by adding 1.0 M NaOH. It is important to note that the solutions containing MoO_4^{2-} that were dissolved in 1.0 M HNO_3 were made new before running each experiments because Mo(VI) transitions to a more stable form, Mo(IV) in the form of a precipitate, which is not sensitive toward air or aqueous oxidation. A color change from a soluble metallic gray to a white precipitate in the solution of MoO_4^{2-} signaled this change after the solutions were left to sit overnight. Mo(IV) does not undergo

disproportionation in aqueous solution and is stable toward air oxidation. At lower acidity an insoluble hydroxide Mo(IV) precipitates, which is why low concentrations (89 mM MoO_4^{2-}) were used.

The reduction of $Mo(VI) \rightarrow Mo(IV) \rightarrow Mo(0)$ involves highly negative potentials with the conversion of MoO_2 to Mo metal observed at - 0.980 V, provided in the following table:

Table 3.2: Table of Molybdenum Redox Reactions [31]

Redox Couple	Half Reaction	$E^0(V)$
MoO_2/Mo^{3+}	$MoO_2 + 2H^+ + e^- \rightarrow Mo^{3+} + 2H_2O$	-0.008
MoO_4^{2-}/MoO_2	$4H^+ + MoO_4^{2-} + 4e^- \rightarrow MoO_2 + 2H_2O$	-0.780
MoO_2/Mo	$MoO_2 + 4H^+ + 4e^- \rightarrow Mo + 2H_2O$	-0.152
Mo^{3+}/Mo	$Mo^{3+} + 3e^- \rightarrow Mo$	-0.2

In aqueous solutions the negative potentials cannot be attained without the side reactions associated with H_2(g) dominating the electrode processes. Metallic molybdenum can only be electrodeposited from aqueous solution as an alloy with Fe, Co, or Ni indicating that MoO_x was deposited onto our substrate surfaces [31]. The Figure3.12, below is the CV's of MoO_4^{2-} on a Pt working electrode at a scan rate of 200 mV/s with the pH adjusted to 0.18.

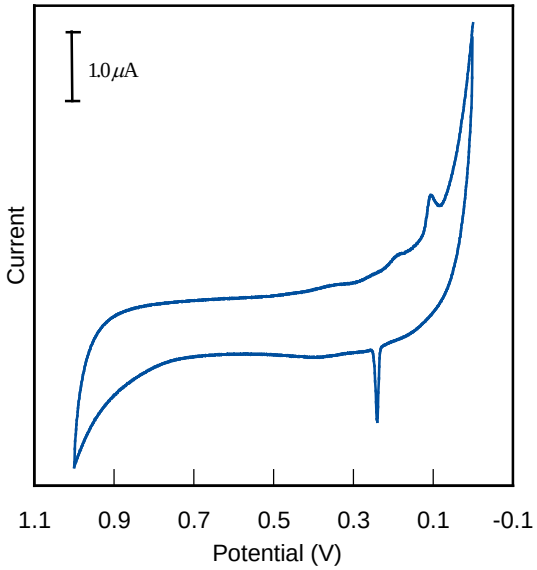

Figure3.12: 0.1 M MoO_4^{2-} Dissolved in 1.0 M HNO_3 and Adjusted to a pH of 0.18 @ 200mV/s on a Pt Working Electrode

From the figure above there is an emergence of a peak at ~ 0.2 V may be associated with an adsorption process with the second peak ~ 0.1 V being an adsorbed layer. Since there might be some Mo(IV) in the solution, it may be a mixture of oxides in the adsorbed layer. Below are the following reactions that may be occurring at the platinum electrode surface:

$$4H^+ + MoO_4^{2-} + 4e^- \rightarrow MoO_2 + 2H_2O$$

$$MoO_2 + 2H^+ + e^- \rightarrow Mo^{3+} + 2H_2O$$

$$MoO_2 + 4H^+ + 4e^- \rightarrow Mo + 2H_2O$$

$$Mo^{3+} + 3e^- \rightarrow Mo$$

Since MoO_4^{2-} will convert to MoO_2 in aqueous solution, the electrochemical responses of MoO_2 were examined. Below is the optimization treatment of the solution parameters:

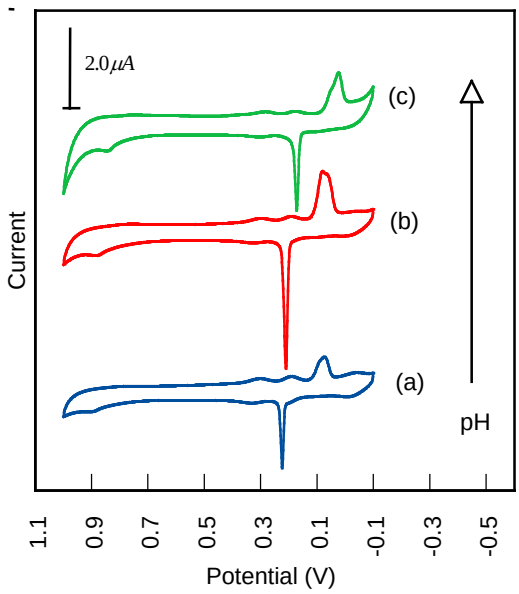

Figure 3.13: 0.01 M MoO_2 Dissolved in 1.0 M HNO_3 with Increasing Aliquots of 1.0 M NaOH on Au Working Electrode at a Scan Rate of 100 mV/s

In Figure 3.13 the potential window is slightly more negative. This may allow for further reduction of Mo species that are adsorbed on the surface of the electrode. Figure 3.12(a) has 0 µL of NaOH and there are reduction peaks ~ 0.3V, 0.2V and 0.09V, along with one large oxidation peak at 0.25V. As the aliquots increase there is resolution between the peaks, until the Figure 3.13(c) with 400 µL. In Figure 3.13(b) there is most resolution in the reduction peaks. It is important to note the increased resolution of the reduction peaks before 0.0 V. This resolution is increased, compared to those scans for Pt, because the H_2(g) reaction is not present in this response.

The electrochemistry of Mo(VI) and (IV) has not been widely studied, however, these CV's are a good beginning to understanding the reduction mechanism. It can be

concluded that there various limitations for depositing Re(0) and Mo(0) from an aqueous system, namely pH, solution conditions, and potential range of the substrate metals. In the following chapter these parameters will be further examined with a non-aqueous system, eliminating the limiting parameters encountered in this chapter.

CHAPTER 4:

ELECTROCHEMISTRY OF RHENIUM AND MOLYBDENUM IN ROOM TEMPERATURE IONIC LIQUID

4.1 MOTIVATIONAND INTRODUCTION

The role of solution pH and electrode composition, aqueous potential window, and side reactions in resolving the electrochemistry of Re and Mo was examined in the previous chapter. This chapter expands the electrochemical studies to include purely ionic, non-aqueous solutions to minimize the limitations associated with the reduction of Re and Mo in aqueous solution. The goal of these studies is to expand the electrochemical analysis into systems that minimize the role of pH and aqueous side reactions to achieve the reduction of oxidized forms of Re and Mo to metal. Specifically, room temperature ionic liquid (RTIL) will be utilized in these studies because the system does not require supporting electrolyte and has very little water that can influence the reduction of either Re or Mo species. The RTIL utilized in these studies will refer to the n-trimethyl-n-propylammnonium cation and the bis(trifluoromethanesulfonyl) imide anion, unless the specific cation [Me_3NPr^+] or anion [$TFSI^-$] is discussed.

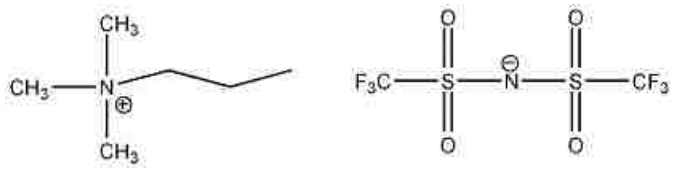

Figure 4.1: Cation/Anion for RTIL, n-trimethyl-n-propylammonium bis-(trifluoromethanesulfonyl) imide.

The solution parameters for the aqueous system were limited by the side reactions including $H_2(g)$ evolution and water oxidation. The inherent physical properties associated with the reduction of the $[Me_3N^+Pr]$ cation and oxidation of $TFSI^-$ anion defines the potential window for the RTIL system. The potential window for electrochemical experiments is expanded relative to water because the oxidation/reduction reactions in aqueous solutions are eliminated and the reduction of the cation and oxidation of the anion occur at great negative and positive potentials, respectively. The more negative potentials that can be attained are well within the potential range for the reduction of both rhenium and molybdenum to metal. Furthermore, in this chapter there will be a discussion expanding on the concept of pH and acidity in RTIL with respect to the electrochemical reduction of rhenium and molybdenum. This discussion is required because the concept of pH in RTIL is not clearly defined or understood relative to the concept of solvation, hydration, and activity aqueous solution.

4.1.1 RTIL Composition and Acidity

It has been established that in our system pH is an integral part of the reduction of ReO_4^-, however in RTIL pH cannot be defined because the activity or concentration of H^+ is not defined in purely ionic solution. In aqueous systems the basic definition of pH is the negative logarithm of the H^+ concentration.

$$\text{pH} \approx pH \approx -\log[H^+]$$

More specifically, the real definition of pH involves the measurement of activity of H^+:

$$pH = -logA_{H^+} = -\log[H^+]\,\Upsilon_{H^+}$$

When pH is measured using a pH meter, the negative logarithm of the hydrogen ion activity is measured rather than the concentration [40]. Typically experiments are conducted such that the activity coefficient of a given species is unity so the measurement can be related directly to the concentration of H^+. The coefficient, γ, can be calculated using the Debye-Hückel equation using the ionic strength, μ, and the hydration sphere, α, for a given ion with charge, z:

$$\log \Upsilon = \frac{-0.51z^2\sqrt{\mu}}{1+\frac{\alpha\sqrt{\mu}}{305}} \text{ @ } 25^{o}\text{C}$$

This equation is valid in aqueous solution of ionic strength $\mu \leq 0.1$ M. If the size parameter is not known then the Davies equation may be used:

$$\log \Upsilon = -0.51z^2\left(\frac{\sqrt{\mu}}{1+\sqrt{\mu}} - 0.3\mu\right) \text{ @ } 25℃$$

This equation is applicable for ionic strength at or below 0.5 M, in our system the ionic strength of the RTIL is 3.77 M. In order to find activity coefficients for ionic strengths above 0.5 M the Pitzer equations may be considered. However, this equation is for aqueous solutions and has not been considered for RTIL solutions:

$$ln\gamma = -A_{\Phi}\left[\frac{I^{1/2}}{1+1.2I^{1/2}} + \left(\frac{2}{1.2}\right)\ln\left(1+1.2I^{1/2}\right)\right] + I\left[(1+y)B_{ReO_4^-} + (1-y)(B_{RTIL}+\theta)\right] + I^2\left[yB'_{ReO_4^-} + (1-y)B'_{RTIL}\right]$$

$$B_j = \beta_j^{(0)} + \beta_j^{(1)}g(I)$$

$$B'_j = \left(\frac{\beta_j^{(1)}}{2I^2}\right)\left[-1+(1+2I^2+2I)\exp(-2I^{1/2})\right.$$

In this equation, y is the solute fraction of the solute, A_{Φ} is the Debye –Hückel parameter, $\beta_j^{(0)}$and $\beta_j^{(1)}$ are the two parameters related to the short-range forces between cations/anions, and I is the ionic strength [40, 41]. However, the equations again used an estimate for the activity coefficient. Furthermore, in our system the ionic strength for the RTIL is 2.147 (using the Davies equation), so it becomes difficult to use any of the

conventional equations that define pH and ionic strength. For solutions with high activities solvation of proton or hydroxyl ion are categorized as non-ideal media, for which the Debye-Hückel equation is no longer valid. For example, values of $-loga_{H^+} = -10$ have been reported for organic systems[42]. In other cases of high acidity systems Hammet Functions have been used. These functions are based on concentrations of protonated/unprotonated forms of the species in solution. The measurement of concentration is from specific "Hammet indicators" that allow for spectroscopic measurement to determination of concentration. These values are obtained under the assumption that the ratio of their activity coefficients remains constant. This is important because the spectroscopic measurements determine concentration rather than activities and can be applied to different acidity functions[42].

4.2Introduction of Electrochemistry in RTIL

Background CVs must be obtained for the RTIL using the different working electrodes that will be utilized in the studies so that reduction processes for Re and Mo can be identified. For example, the voltammetric responses for Pt, Au, and glassy carbon (GC) electrodes in RTIL are provided in Figure 4.2.

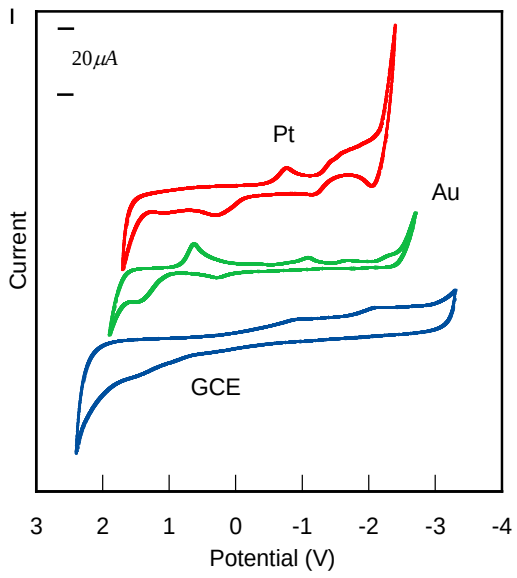

Figure 4.2: Cyclic Voltammetry for Pt, Au, and Glassy Carbon (GC) Electrodes in RTIL.

The voltammetry in Figure 4.2 is significantly different for each different working electrode indicative of cation/anion reactivity at the different materials. For Pt the oxidation and reduction of RTIL at the electrode is significantly detailed relative to either Au or GC. However, oxidation/reduction at Au is also observed possibly due to formation of AuO_x at the electrode surface. The oxidation/reduction of the RTIL significantly diminished for GC in comparison to the metal electrodes because the electrode does not form oxides. The electrochemical window is expanded for all electrode studied in RTIL when compared to aqueous system. This is specifically attributed to a lack of side reactions associated with water and the formation of oxides at the metal electrode surfaces. As a consequence, the potential window is expanded to sufficiently negative potentials that encompass the reduction of Re and Mo to metal.

The potential window associated with each working electrode in RTIL is summarized in Table 4.1.

Table 4.1: Potential Windows for Pt, Au, GCE Electrodes for Aqueous and RTIL Systems

Substrate Metal	Aqueous Potential Window	Non-Aqueous Potential Window
Platinum	1.0 V – 0.0 V	1.7 V – (-2.4 V)
Gold	1.0 – (-0.1 V)	1.9 V – (-2.7 V)
Glassy Carbon	N/A	2.6 V – (-2.7 V)

The role of proton adsorption at the Pt working electrode was important for the reduction of Re based on the schematic present below where perrhenate is reduced through Re oxide to metal. We found that in aqueous solutions the surface deposit was predominantly the oxide with no measurable Re metal on the surface of the electrode, which is verified by previous studies to ensure that H^+ is available in the RTIL system the acid form of the anion (HTFSI) is directly dissolved in the RTIL.

$$ReO_4^- \xrightarrow{E_1} ReOx_{(ad)} \xrightarrow{E_2} Re$$

The reduction of ReO_4^- in RTIL may follow the same mechanism established in aqueous solution. The following electrochemical half-cell reactions for Re and Mo are provided for reference:

$$ReO_4^- + 8H^+ + 7e^- \rightarrow Re + 4H_2O$$

$$ReO_4^- + 4H^+ + 3e^- \rightarrow ReO_2 + 2H_2O$$

$$ReO_2 + 4H^+ + 4e^- \rightarrow Re + 2H_2O$$

$$MoO_2 + 4H^+ + 4e^- \rightarrow Mo + 2H_2O$$

$$MoO_4^{2-} + 8H^+ + 6e^- \rightarrow Mo + 3H_2O$$

$$H_2O \rightarrow H^+ + OH^-$$

In addition, the water dissociation reaction is included because there is a small amount of water in the RTIL (200 ppm) that may provide H^+. In contrast to the aqueous electrochemistry where the pH could be controlled and measured precisely, the trace amounts of H_2O in the RTIL may dissociate and provide the H^+ needed to initiate the reduction of Re and Mo. However, the concentration is small and may not be sufficient to sustain the electrochemical reduction of Re and Mo in the RTIL without the addition of HTFSI. Therefore, the electrochemical reduction Re and Mo in RTIL will be conducted with and without the addition of acid HTFSI.

4.2.1 Rhenium Electrochemistry in RTIL

The electrochemical response of a Pt electrode in RTIL solution containing 89 mM ReO_4^- without additional acid is provided in Figure 4.3. The solutions were sonicated to ensure the complete dissolution of the Re in RTIL. The RTIL background is plotted with the cyclic voltammetry of ReO_4^- for clarity.

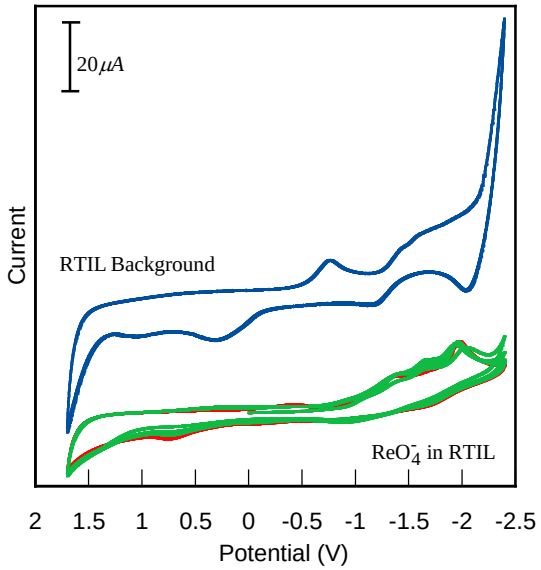

Figure 4.3: Voltammetric Response of a Pt Working Electrode in Solution Containing 89 mM ReO_4^- Dissolved in RTIL. Scan rate = 100 mV/s.

The background cyclic voltammetry is obtained using the potential window between+1.7 V and -2.4 V. The cyclic voltammetry for the Pt electrode in 89 mM ReO_4^- in RTIL is significantly different. Specifically, the reduction at ~-0.7 and between -1.5 and 2.4 is diminished relative to the background. The electrochemistry changes due to the fact that the reduction of Re is more favorable than reduction of the RTIL cation at the Pt surface. Thus, the voltammetry for the reduction of the cation is significantly diminished. In addition, the voltammetry may be influenced by the reduction of Re at the electrode surface, changing the composition and diminishing the reduction of the cation. The negative potentials utilized to obtain the cyclic voltammetry allow the reduction of ReO_4^- to Re metal. There are three reduction waves at -0.5 V, - 1.35 V, and - 2.0 V. The voltammetric wave at – 0.5 V may be attributed to the uptake of H^+ at the Pt surface from residual water. However, this potential is the reduction peak at -1.35 V can likely be

attributed to the reduction of ReO_4^- to for the ReO_2 intermediate on the Pt surface. The peak at – 2.0 V would then be associated with the reduction of the ReO_2 to Re metal on the Pt surface.

Similar voltammetry is obtained when examining the reduction of ReO_4^- at the gold electrode surface. The cyclic voltammetric response on a gold working electrode is presented for a solution containing 89 mM ReO_4^- in RTIL.

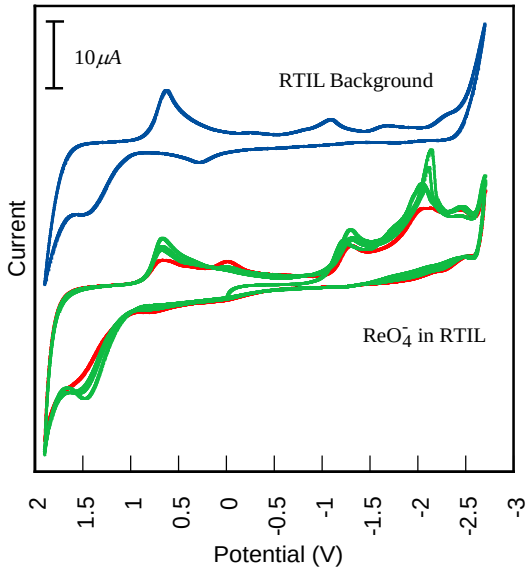

Figure 4.4: Voltammetric Response of a Au Working Electrode in Solution Containing 89 mM ReO_4^- Dissolved in RTIL. Scan rate = 100 mV/s.

There are again three reduction peaks that occur at - 1.35 V, -2.0 V, and -2.4 V. The current for the reduction of ReO_4^- at the gold working electrode was enhanced relative to Pt in RTIL. The trend was reversed in aqueous solution with the reduction of ReO_4^- significantly enhanced relative to Au based on the adsorption of proton and the

subsequent use of H_{ads} as a reducing agent in aqueous solution. Although it is likely that the reduction of ReO_4^- is tied to proton concentration in RTIL the adsorption of H^+ at the electrode surface does not dominate or enhance the reduction processes. The reduction likely occurs through the same process observed at the Pt electrode. However, additional reduction processes are possible provided there is sufficient water and proton available in the RTIL based on the following reactions:

$$ReO_4^- + 8H^+ + 7e^- \rightarrow Re + 4H_2O \ (E^o = 0.34\,V)$$

$$ReO_4^- + 4H^+ + 3e^- \rightarrow ReO_2 + 2H_2O \ (E^o = 0.51\,V)$$

Finally, the electrochemistry on a glassy carbon is provided for comparison to both Au and Pt. The use of GC is important because it is not metallic and compared to both Pt and Au it is catalytically inert further minimizing the oxidation/reduction of the anion/cation of the RTIL, respectively. The voltammetric response of the GC electrode in a solution containing 89 mM ReO_4^- dissolved in RTIL is presented in Figure 4.5.

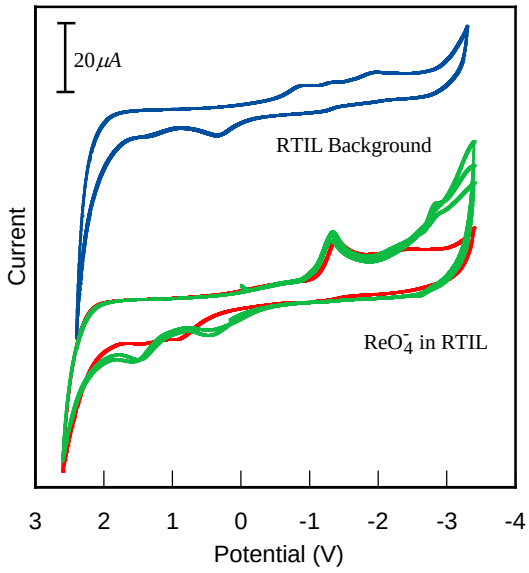

Figure 4.5: Voltammetric response of a GC Working Electrode in Solution Containing 89 mM ReO_4^- Dissolved in RTIL. Scan rate = 100 mV/s.

The potential window for GC is significantly larger than Pt and Au. The GC electrode is inert relative to Pt and Au and there is a reduction wave at - 1.2 V followed by broad reduction more negative of -2.0 V. The voltammetry is consistent with the reduction of Re to metal without resolution of the reduction of intermediate species such as ReO_2. The voltammetry for all three electrodes studies suggest that the reduction of ReO_4^- occurs without additional H^+ in the RTIL solutions. The question remains whether the voltammetry is still tied to the proton adsorption at Pt and Au that would be available from the dissociation from residual water in the RTIL.

4.2.2 Electrochemistry of ReO_4^- in RTIL containing HTFSI

The importance of acidity of the solution has been established as being a crucial component for the targeted ReO_4^- reduction in aqueous solution at Pt and Au electrodes. Introducing protons in the non-aqueous system is achieved using HTFSI, the acid anion of the RTIL. The experiments were conducted in the same manner as the aqueous solutions. Specifically, aliquots of the HTFSI (which will be referred to as Ac-RTIL) were added to the RTIL solution containing ReO_4^- until the electrochemistry was resolved and optimized. This treatment is shown for only Au but first will be the discussion of the electrochemistry with the Ac-RTIL treatment for the platinum working electrode, Figure 4.6.

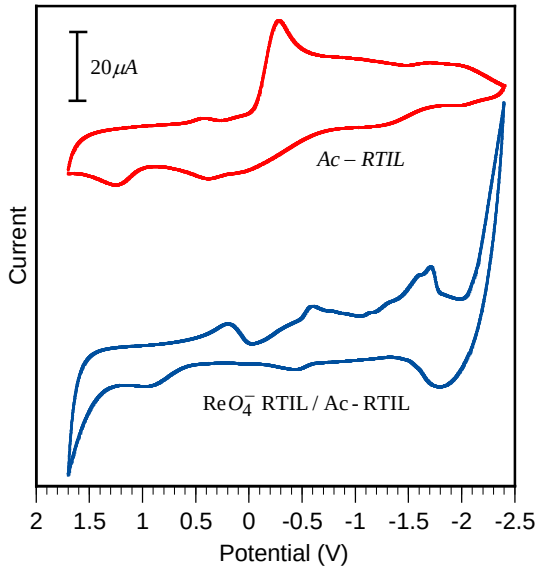

Figure 4.6Voltammetric Response of a Platinum Working Electrode in Solution Containing 89 mM ReO_4^-Dissolved in RTIL with 4.0 mL of 1.0 M HTFSI. Scan rate = 100 mV/s.

The cyclic voltammetric responses for the Ac-RTIL and ReO_4^- RTIL/Ac-RTIL are very different, compared to the CVs obtained in pure RTIL. There are multiple reduction peaks that are observed at – 0.6 V, - 1.5 V, - 1.7 V. These reduction peaks can be associated with the reduction of ReO_4^- to the intermediate of ReO_2, and then Re. The CV response with Ac-RTIL is greater than that with none added. This increase of response could be due to the addition of H^+; which can lead to greater H_{ad} on the surface of the Pt working electrode. Another possibility to the increase in response could be because of the half-cell reactions, which require H^+ to occur:

$$ReO_4^- + 8H^+ + 7e^- \rightarrow Re + 4H_2O \ (E^o = 0.34\,V)$$

$$ReO_4^- + 4H^+ + 3e^- \rightarrow ReO_2 + 2H_2O \ (E^o = 0.51\,V)$$

$$ReO_2 + 4H^+ + 4e^- \rightarrow Re + 2H_2O \ (E^o = 0.252\,V)$$

However, the response on Pt is still larger than that of Au, which can be seen below. The cyclic voltammetry below examines the influence of increasing acid HTFSI on the reduction of ReO_4^- in RTIL at the gold working electrode. The goal is to determine the concentration range where the largest relative reduction of Re can be observed.

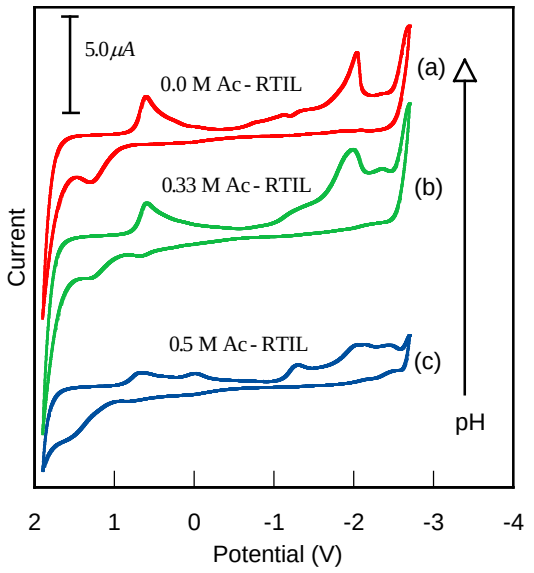

Figure 4.7: Voltammetric Response of a Gold Working Electrode in Solution Containing 89 mM ReO_4^- Dissolved in RTIL. Scan rate = 100 mV/s.

It is clear in Figure 4.7 that as the concentration of the Ac-RTIL increases there is a loss resolution of the voltammetric response. The electrochemistry for the reduction of Re without acid is shown in Figure 4.7a for comparison. The voltammetry shows reduction starting at -1.0 V with resolved peaks at ~ -2.4 V. The peak at ~ -2.4 V is significantly diminished once an acid concentration of 0.5 M in RTIL is reached (Figure 4.7c). There is also a slight loss in the resolution of the two peaks at – 1.0 V and – 1.4 V

when the concentration of acid is 0.33 M (Figure 4.7 b). However, the overall magnitude of the current is the highest at the concentration of acid. The data suggests that acid concentration is again critical in the reduction of the Re species at the Au electrode.

The evolution of the cyclic voltammetry for the reduction of ReO_4^- is shown in Figure 4.8. The first scan (red) shows the initial reduction of Re at the Au surface. With each additional scan the current is slightly diminished due to electrochemical deposition of Re. The large peak at – 2.7 V looks similar to the bulk deposition peaks found in aqueous systems and can be attributed to the reduction of ReO_4^- to ReO_2 and possibly Re(0). The final CV scan is graphed as the purple scan, taken at steady state. Without graphing the preceding CV scans it would difficult to observe the progression of the changes due to the reduction of Re.

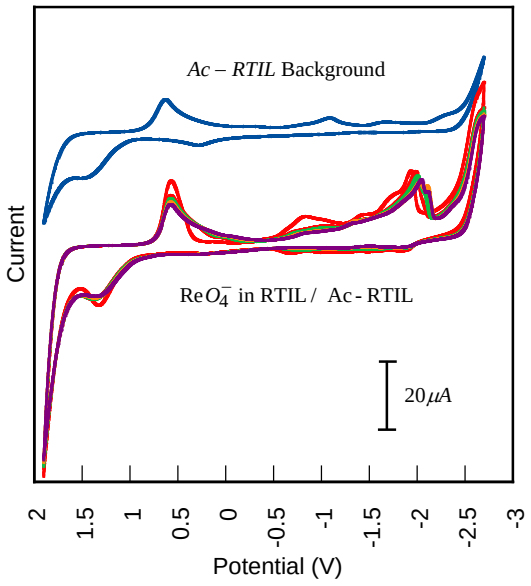

Figure 4.8: Voltammetric Response of a Gold Working Electrode in Solution Containing 89 mM ReO_4^- Dissolved in RTIL with 0.33 M HTFSI. Scan rate = 100 mV/s.

The SEM image shows the Re aggregates from the electrochemical reduction of ReO_4^-.

Figure 4.9: SEM Data of Au Deposited from 0.089 M ReO_4^- dissolved in RTIL with 4.0 mL of HTFSI

Chemical analysis using EDS was obtained for the deposits shown in the image (Figure 4.9) with the areas of interest shown below in Figure 4.10.

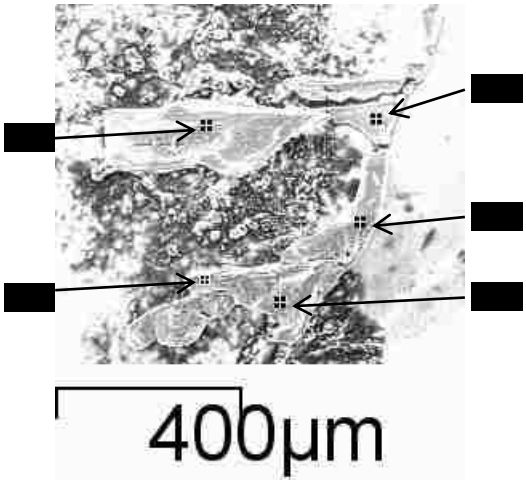

Figure 4.10: SEM Picture of the Area of Interest Scanned for EDS Data

All of the EDS data collected for sites shown confirm the deposition of Re on the surface of the gold electrode. A representative EDS spectrum is provided in Figure 4.11.

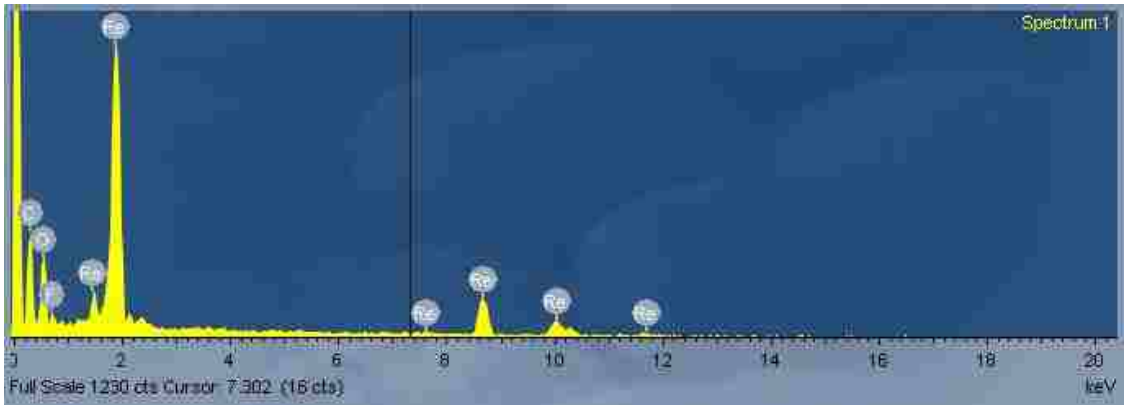

Figure 4.11: EDS for the Corresponding SEM Data: 1

The spectra indicates that the presence of Re on the surface. Also, it indicates that oxygen was present. The source of oxygen may be from exposure to normal atmosphere forming a surface oxide on Re. However, the source may also be an unreduced ad-layer of ReO_2 present at the electrode surface. Further studies are required to determine if the all of the Re deposited can be fully reduced to metal. However, the concentration of oxygen from EDS is sufficiently small relative to the Re concentrations to infer that some of Re is in metallic form.

Finally a voltammetric response was taken with the glassy carbon working electrode, which is shown below (Figure 4.12). The reduction of Re at the GC electrode is significantly different than both the Pt and Au electrodes. The voltammetry is diminished relative to the more noble metal electrodes utilized. However, the potential window for GC is significantly larger than both Au and Pt.

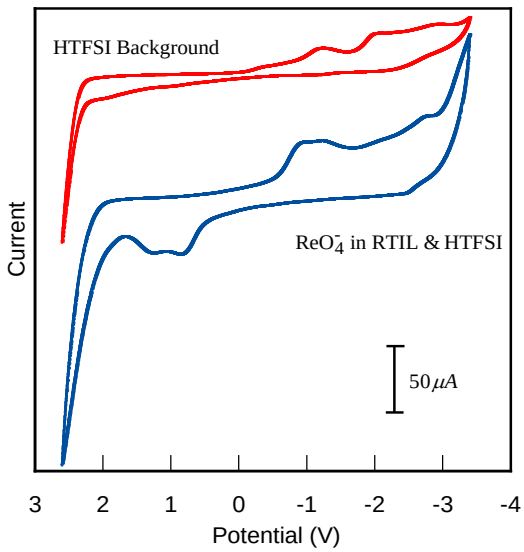

Figure: 4.12 Voltammetric Response of a GC Working Electrode in Solution Containing 89 mM ReO_4^- Dissolved in RTIL with 4.0 mL of 1.0 M HTFSI. Scan rate = 100 mV/s.

There is also minimum activity associated with the reaction of the RTIL at the GC electrode at negative potentials which allows the voltammetry associated with the reduction of Re to be clearly observed. The mechanism for the reduction of Re at GC is not well understood because the adsorption of H^+ at the GC surface is not prominent. Therefore, the role it plays in the reduction is questionable. Therefore, the role of H_{ad} adsorbed on the surface will not aid in the reduction of Re precursors to Re(0).

The role of acid is clearly distinguished in the voltammetry at Pt and Au electrodes. Increasing the acid in the RTIL provides enhanced current responses associated with the reduction of Re at both of these electrode surfaces. However, diminished voltammetry was observed indicating there is a limit associated with increasing acid. The data again supports the role of acid in the reduction of ReO_4^- within certain concentrations limits. In addition, it suggests that the reduction is a multi-step process that is strongly dependent on the available acid in the RTIL. In contrast to aqueous solution the evolution of hydrogen gas in RTIL is not observed which suggests that the Pt and Au surface may get blocked by adsorbed H_{ads} on the surface of the electrode, minimizing the further reduction of Re at higher acid concentrations.

4.3 Electrochemistry of Molybdenum in RTIL Solution.

4.3.1 Introduction

The information gathered from analyzing the electrochemical reduction of Mo could be used in conjunction with the perrhenate studies to define technetium recovery using RTIL solutions. However, there are few examples that provide details regarding the

electrochemical behavior of molybdenum in either aqueous or non-aqueous solutions. The half-cell reactions of known reduction pathways for Mo are reported from aqueous environments are provided in Table 4.2 and it is assumed that the species will behave similarly in non-aqueous system including RTIL:

Table 4.2: Redox Couples, Half-Cell Reactions, and E^o for Molybdenum [31]

Redox Couple	Half Reaction	$E^0(V)$
MoO_2/Mo^{3+}	$MoO_2 + 2H^+ + e^- \rightarrow Mo^{3+} + 2H_2O$	-0.008
MoO_4^{2-}/MoO_2	$4H^+ + MoO_4^{2-} + 4e^- \rightarrow MoO_2 + 2H_2O$	-0.780
MoO_2/Mo	$MoO_2 + 4H^+ + 4e^- \rightarrow Mo + 2H_2O$	-0.980
Mo^{3+}/Mo	$Mo^{3+} + 3e^- \rightarrow Mo$	-0.2
MoO_4^{2-}/Mo	$MoO_4^{2-} + 6e^- + 8H^+ \rightarrow Mo + 4H_2O$	-0.913

In addition, the following oxidation/reduction flow chart for possible Mo in aqueous solution is provided for clarity:

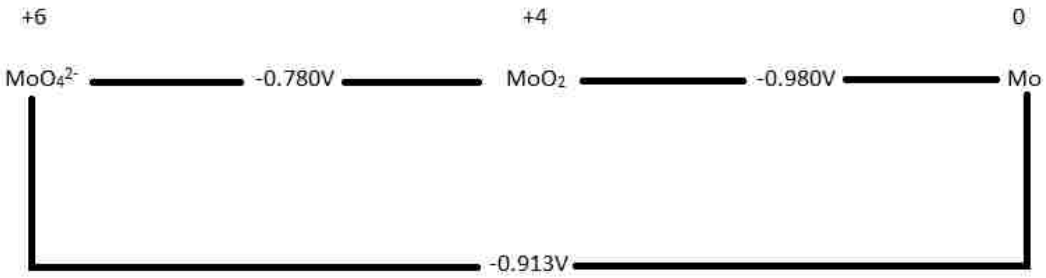

Figure4.13: Molybdenum Oxidation State Flow Chart

The Mo species analyzed in this work were in the form of MoO_4^{2-} and $MoO_2$to provide the two different oxidations states (Mo^{6+} and Mo^{4+}) of the species in RTIL. In the previous chapter it was mentioned that in aqueous solutions, Mo forms various complexes depending on the species in the solution and the acidity (pH). In contrast to the dissolution of MoO_4^{2-} and MoO_2which changed colors due to complexation and chemical change in aqueous solution, when Mo species were dissolved in RTIL there was an increase in solubility and the solutions did not undergo color change. The data suggests that Mo species dissolved in the RTIL do not form complexes that change the overall chemistry of the species. Solutions were allowed to sit for a week and replicate measurements were taken over this period of time to confirm the stability of the solution species.

4.3.2 Electrochemical Reduction of MoO_4^{2-} and MoO_2 in RTIL

The electrochemical reduction of MoO_4^{2-} was studied under the same conditions as perrhenate, with a starting solution of89 mM MoO_4^{2-} dissolved in RTIL. Voltammetric responses were obtained using Pt, Au, and GC working electrodes. The voltammetric

responses for the MoO_4^{2-} and MoO_2 dissolved in RTIL solution are shown for a platinum working electrode below in Figure 4.14.

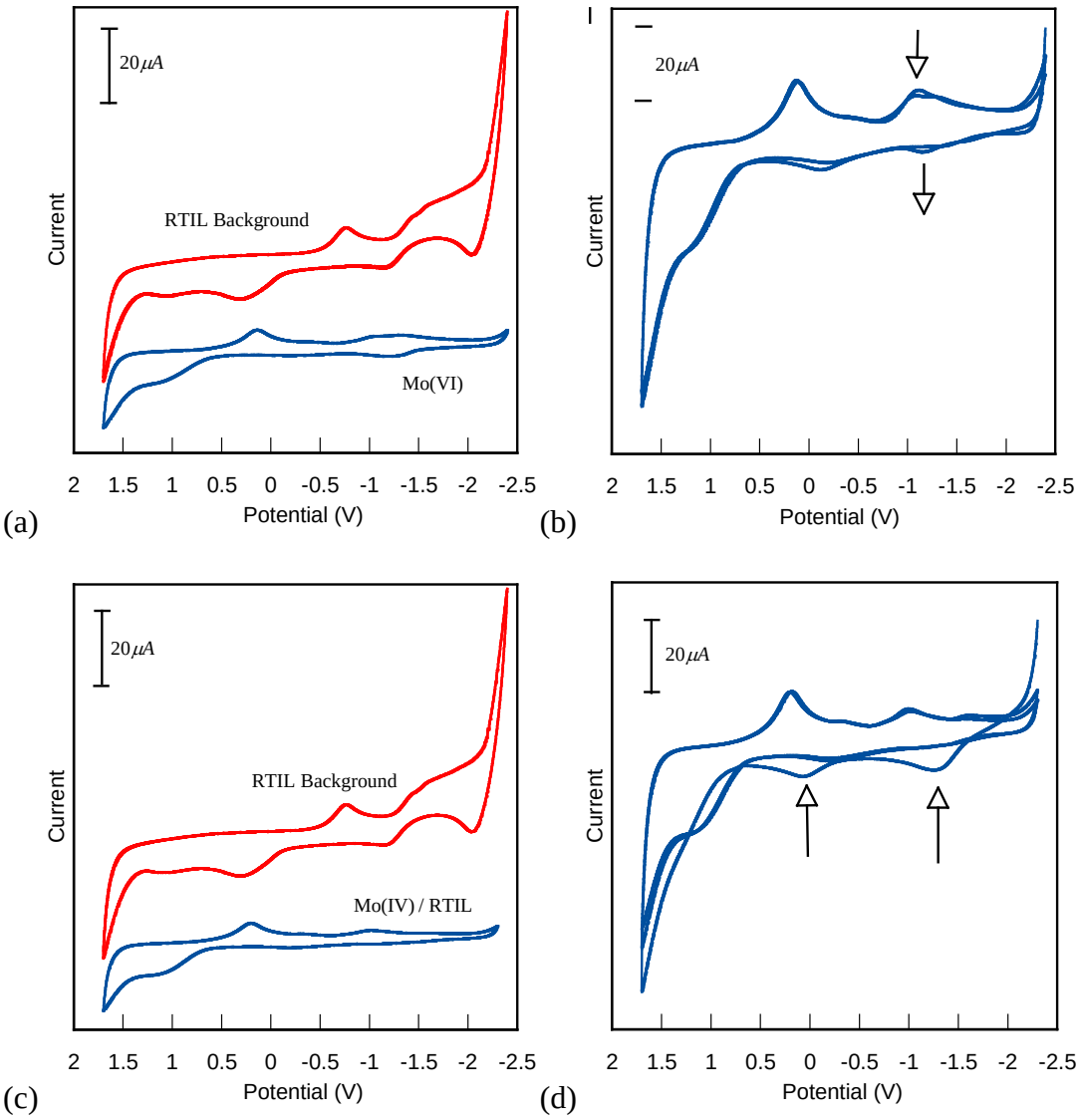

Figure 4.14 (a, b): Voltammetric response of a platinum working electrode in solution containing 89 mM MoO_4^{2-} dissolved in RTIL. Scan rate = 100 mV/s. A, is the RTIL background with steady state scan for Mo(VI) in RTIL. B is the progression scans for Mo(VI). Figure 4.14 c, d : Cyclic voltammetric response of platinum working electrode in a solution containing 89 mM MoO_2dissolved in RTIL; C, is the RTIL background and the steady state scan of Mo(IV) in RTIL. D is the progression scan of Mo(IV) in RTIL.

The voltammetry associated with MoO_4^{2-} is significantly different from the background associated with the RTIL (Figure 4.14a). Specifically the reduction of the cation is suppressed for Mo(VI) in comparison to pure RTIL. The data suggests that the reduction of Mo(VI) is more thermodynamically favorable in comparison to the RTIL cation. The emergence of a reduction peaks ~0.1 V and ~ -1.2 V for MoO_4^{2-} are observed, in both 14.4a, b. The voltammetry associated with the reduction of Mo(VI) is reduced relative to Re indicating that the relative reactivity of the species is diminished at the Pt electrode. The response gradually decreases until a steady state is reached (4.14a). The decrease in reduction may be associated with the deposition of Mo on the Pt surface. The initial scans are shown, 4.14c, and the steady state 4.14d. Similarly to MoO_4^{2-}, the voltammetric response is diminishes as the scans progress. This indicates that there are changes occurring on the surface of the electrode. The surface adsorption of proton may minimize the reduction of Mo because hydrogen gas is not evolved under the electrochemical conditions utilized in these studies. The half-cell potentials for Mo indicate that reduction will occur at very negative potentials (~ -0.9 V). It is most likely that Mo(VI) is being reduced through the following reactions:

$$4H^+ + MoO_4^{2-} + 4e^- \rightarrow MoO_2 + 2H_2O \ (E^o = -0.780\ V)$$

$$MoO_2 + 2H^+ + e^- \rightarrow Mo^{3+} + 2H_2O \ \ (E^o = -0.008\ V)$$

$$MoO_2 + 4H^+ + 4e^- \rightarrow Mo + 2H_2O \ (E^o = -0.980)$$

$$Mo^{3+} + 3e^- \rightarrow Mo \ (E^o = \ -0.2\ V)$$

$$MoO_4^{2-} + 6e^- + 8H^+ \rightarrow Mo + 4H_2O \ (E^o = \ -0.913)$$

The reduction to Mo metal could not be achieved in aqueous solution because the negative potentials could not be attained before the hydrogen evolution dominates other possible reactions at the electrochemical surface. In contrast, the expanded negative potentials associated with RTIL solutions allows the reduction of Mo(IV) to metal.

For comparison the electrochemistry is analyzed for MoO_4^{2-} at a gold working electrode shown in Figure 4.15.

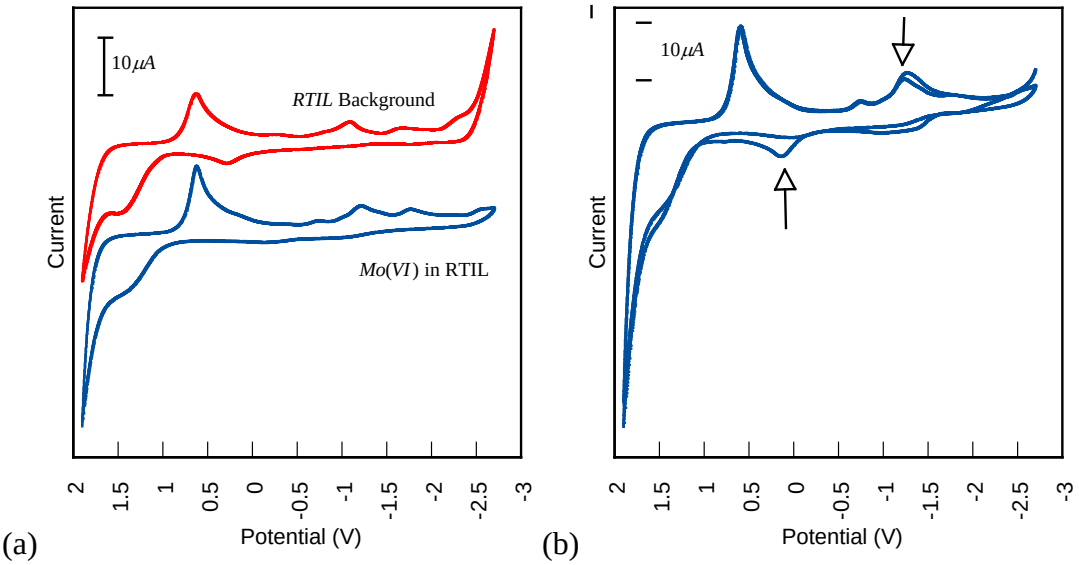

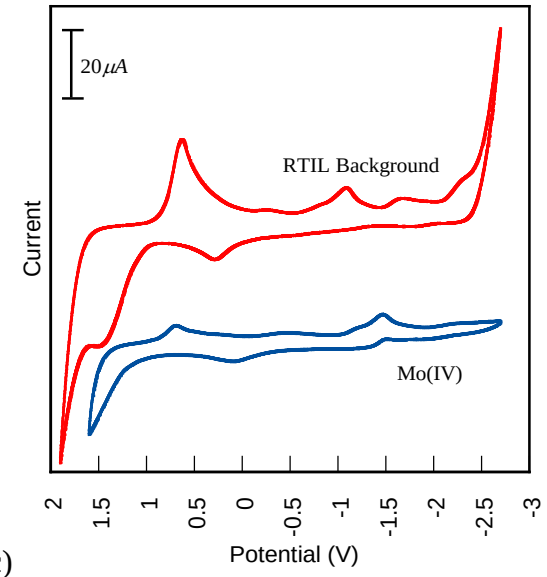

(c)

Figure 4.15 a, b: Cyclic voltammetric response of gold working electrode in a solution containing 89 mM MoO_4^{2-} in RTIL. Figure 4.15a: is the RTIL background with Mo(VI) steady state scan. Figure 4.15b: progression scans for Mo(VI) in RTIL. Figure 4.15c: Voltammetric response of gold working electrode in a solution containing 89 mM MoO_2dissolved in RTIL.

The steady state scan 4.15a shows a loss of response from the initial scans (Figure 4.15b). This loss of voltammetric response may again be due to a change of the gold electrode as Mo is reduced onto the surface. There are reduction peaks that are absent in the RTIL background, at – 0.9 V and – 1.3 V. These two reduction peaks are likely associated with the reduction of Mo based on the reactions below:

$$4H^+ + MoO_4^{2-} + 4e^- \rightarrow MoO_2 + 2H_2O \ (E^o = -0.780\ V)$$

$$MoO_2 + 4H^+ + 4e^- \rightarrow Mo + 2H_2O \ (E^o = -0.980)$$

$$MoO_4^{2-} + 6e^- + 8H^+ \rightarrow Mo + 4H_2O \ (E^o = -0.913)$$

The cyclic voltammetry in Figure 4.15 does not utilize the maximum potential window in order to minimize the formation of gold oxide at positive potentials. In addition, the potential window utilized minimizes the possible re-oxidation of the Mo

deposits after the reduction processes are completed. When the scans were run at their maximum potential window, there was very large oxidation peak in the positive scan that is eliminated using the modified potential window. Moreover, production of gold oxide could also inhibit the reduction of the Mo species at negative potentials if it remained un-reduced.

The voltammetric response for MoO_2 is lower in comparison to the same concentration of MoO_4^{2-} at the gold electrode in Figures 4.15 a, b, and c. It is possible that the reduction of Mo(VI) is more thermodynamically favorable which suggests that the intermediate species may not be Mo(IV). Thus the reduction of Mo(VI) to Mo(0) is easier to achieve than Mo(IV) to Mo(0). The reduction potential for Mo(VI) is - 0.913 V and -0.980 V for Mo(IV) which supports the assignments based on the thermodynamics associated with reduction of the two species in aqueous solutions.

In addition, the electrochemical response for both Mo species is diminished when compared with Re at the same concentration and at the same electrode. The decrease in response may be due to the various Mo species in the RTIL solution during the reduction processes. The oxidized/reduced forms of Mo in RTIL might be sufficiently stable that reduction is reduced due to kinetic limitations. In the case of Re, the intermediate surface species ReO_2 aides in the reduction to metal. The formation of intermediate surface species of Mo has not been established in ionic liquid solutions. Furthermore, the half-cell potentials for Mo are more negative than those of Re.

Finally the cyclic voltammetric response for a GC electrode was obtained in the same RTIL solution containing 89 mM MoO_4^{2-}.

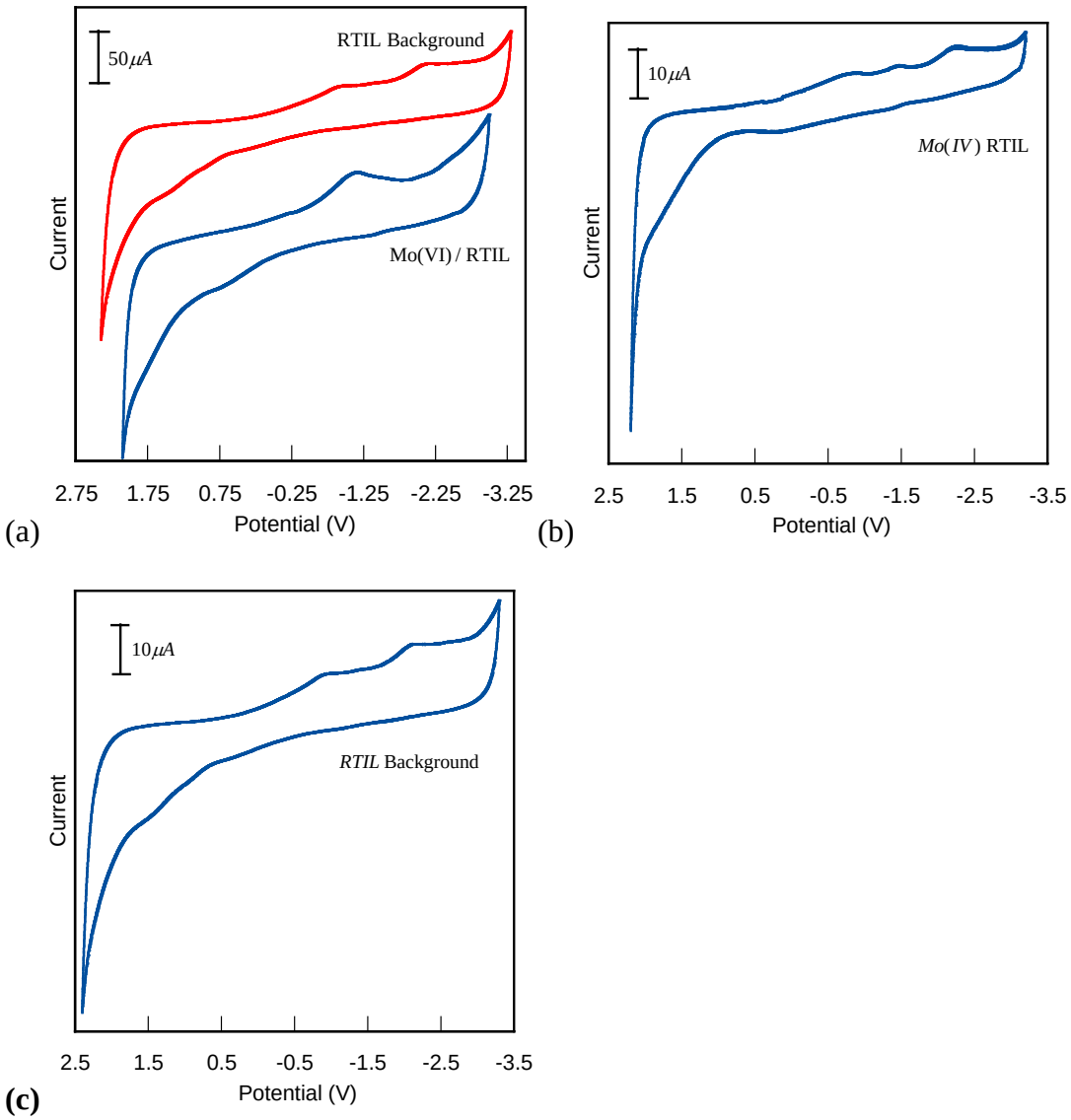

Figure 4.16a: Voltammetric response of a GC working electrode in a solution containing 89 mM MoO_4^{2-} dissolved in RTIL. Figure 4.16b: Voltammetric response of GC working electrode in a solution containing 89 mM MoO_2 dissolved in RTIL.

The response of Mo(VI/IV) is discernable to the RTIL background for Figures 4.16a and 4.16b. The response for Mo(VI) is greater than the background and less for Mo(IV)indicating the thermodynamic properties are different for each Mo species. For

Mo(VI) there is only one reduction peak for the negative scan. In contrast, there are 3 different reduction peaks for Mo(IV). This indicates that the reduction process for Mo(VI) is much simpler compared to Mo(IV). The reduction of Mo(IV) may involve other intermediates that are not present in the reduction pathway associated with Mo(VI). Moreover the direct reduction of Mo(VI) to Mo(0) is more thermodynamically favorable in comparison to the reduction of Mo(IV) to Mo(0) in RTIL. This agrees favorably with the reduction potential observed in aqueous solution which indicates the direct reduction of Mo(VI) to Mo(0) occurs at - 0.913 V compared to the reduction of Mo(IV) to Mo(0) at - 0.980 V.

The half-cell reactions indicate that proton is needed for the reduction of the Mo species. The residual water in the RTIL becomes the only source of the H^+ which may inhibit the reduction of the species at the electrode surface In the following section introduction of HTFS will be examined and the role of H^+ addition will be assessed for the reduction of Mo(VI) and Mo(IV).

4.3.3 Electrochemical Reduction of MoO_4^{2-} MoO_2 in RTIL Containing HTFSI

From the aqueous studies the acidity of the supporting electrolyte was established as an important factor which enhanced the reduction of Re. Therefore H^+ was introduced to the RTIL solution. This resulted in an increase in the solubility of the Mo species and the ultimate concentration that could be achieved in RTIL relative to aqueous solution. However, for the studies presented the concentration of Mo was maintained at 89 mM for direct comparison to previous voltammetry. The CV response for $MoO_4^{2-}$and MoO_2in RTIL containing 0.3 M HTFSI for a platinum working electrode is shown in Figure 4.17.

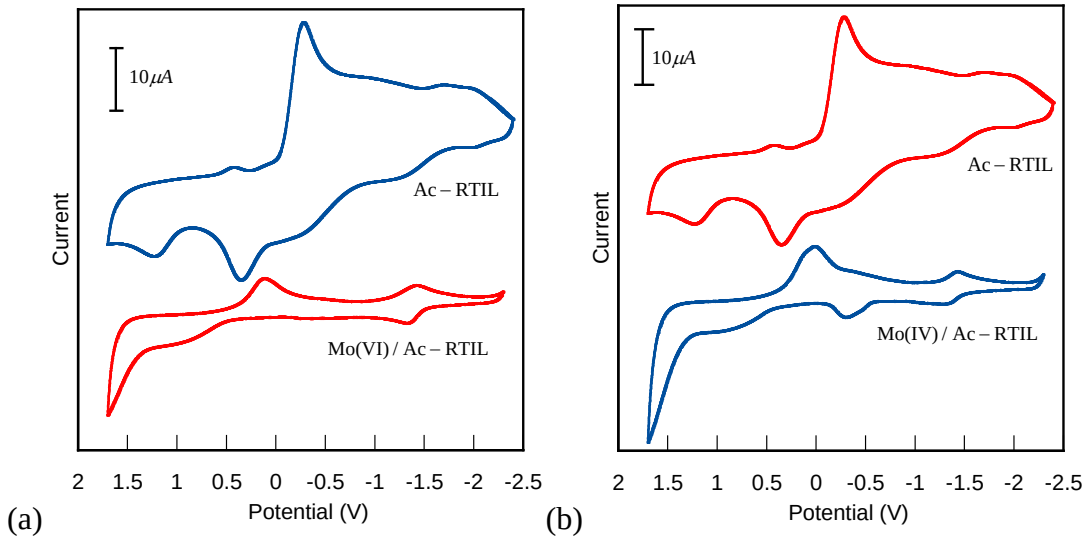

Figure 4.17a. Voltammetric response of Pt working electrode in solution containing 89 mM MoO_4^{2-} dissolved in RTIL with 0.5 M HTFSI. Figure 4.17b: Voltammetric response of a Pt working electrode in a solution containing 89 mM MoO_2dissolved in RTIL with 0.5 M HTFSI.

In Figure 4.17athere is an emergence of a reduction peak ~0.01 V and -1.55 V. The addition of HTFSI with the Pt working electrode resolved the electrochemistry in the MoO_4^{2-} reduction, when compared to the CV with no HTFSI.

The CV response of MoO_2 is more resolved as H^+ is added, compared to the CV with no additional H^+ in the RTIL. There are reduction peaks0.0 V and ~ - 1.4 V. The peak at ~ 0.0 V indicates that the reduction of Mo(IV) to Mo(0) may be occurring through sequential reductions through a Mo(III) intermediate:

$$4H^+ + MoO_4^{2-} + 4e^- \rightarrow MoO_2 + 2H_2O \ (E^o = -0.780\ V)$$

$$MoO_2 + 2H^+ + e^- \rightarrow Mo^{3+} + 2H_2O \ \ (E^o = -0.008\ V)$$

$$Mo^{3+} + 3e^- \rightarrow Mo \ (E^o = \ -0.2\ V)$$

$$MoO_4^{2-} + 6e^- + 8H^+ \rightarrow Mo + 4H_2O \ (E^o = \ -0.913)$$

The second reduction peak can be attributed to the reduction of this species to Mo(0). Oxidation of Mo species is also observed consistent with the oxidation of surface Mo species and the possible oxidation of Mo(IV) to Mo(VI) at ~ - 0.3 V. This voltammetric wave observed in the response for Mo(VI) suggests that the reduction of Mo(IV) occurs through a very different mechanism. The addition of H^+ to the RTIL solution helps the reduction of Mo by suppressing the background reduction of the cation of the ionic liquid. The reduction mechanism may not be the same for the gold working electrode. The cyclic voltammetric scans for MoO_4^{2-} solution dissolved in RTIL with the HTFSI concentration of 0.3 M on a gold working electrode is show in Figure 4.18.

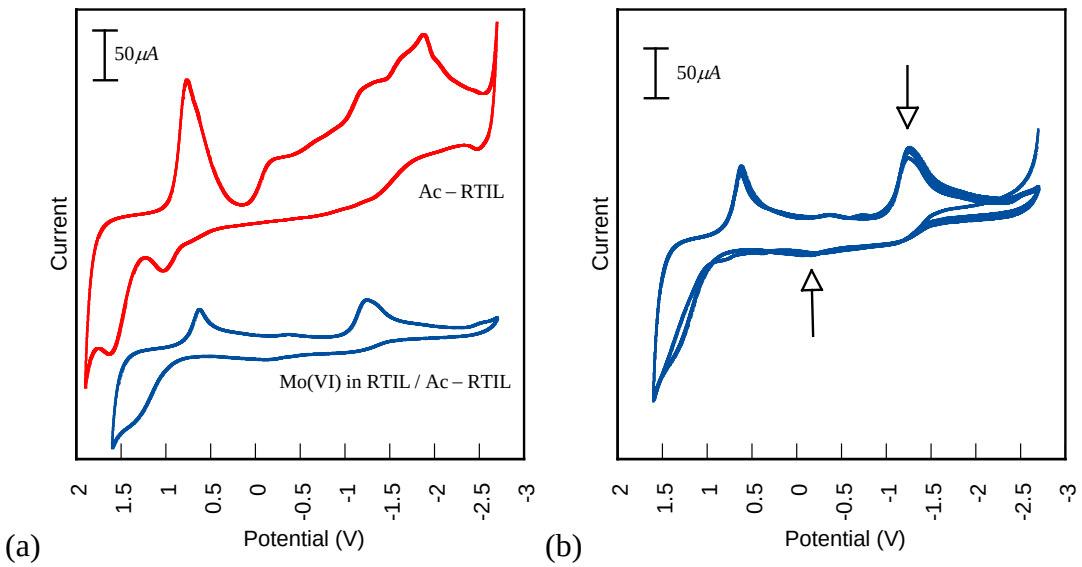

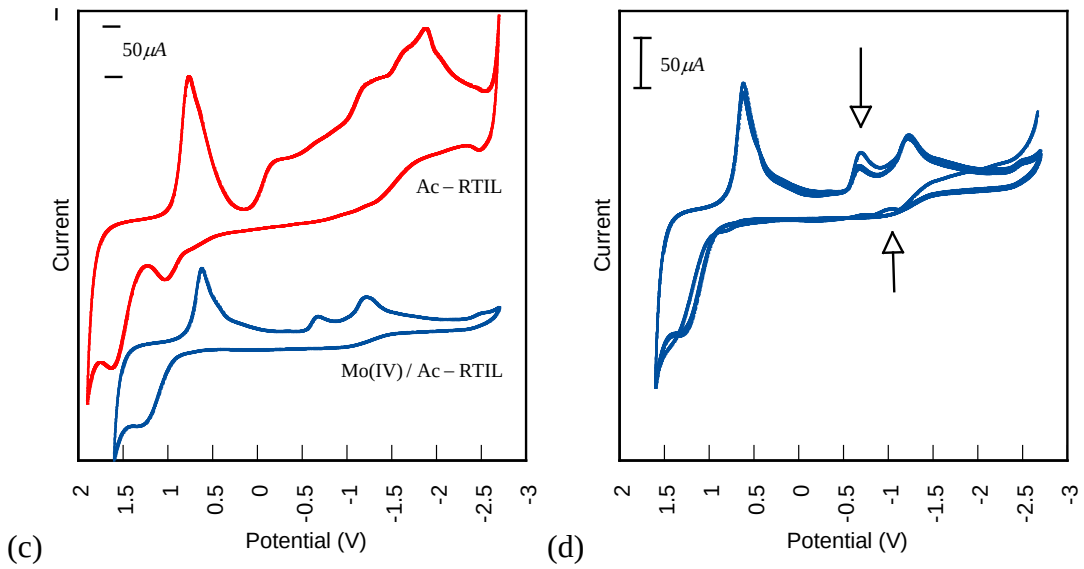

Figure 4.18a, b: 89 mM MoO_4^{2-} Dissolved in RTIL with 2.0 mL of 1.0 M HTFSI on a gold Working Electrode. Figure 4.18a: is the Ac-RTIL background with Mo(VI) steady state. Figure 4.18b is the progression scans. Figure 4.18c, d: Voltammetric response of gold working electrode in a solution containing 89 mM MoO_2 in 0.5 M HTFSI background and steady state scan. Figure 4.18d is the progression scan for Mo(IV) in HTFSI.

For CV in Figure 4.18 a, b there are reduction peaks at ~ – 0.4 V and~– 1.25 V. The first reduction peak may be associated with the reduction of Mo(VI) to Mo(IV) and the second peak to Mo(0). The addition of acid does not significantly enhance the voltammetry associated with the reduction of Mo but it does diminish the reduction of the RTIL cation.

For Figure 4.18 c, d, the reduction peaks at – 0.7 V and – 1.25 V are much more resolved compared to the CV of MoO_4^{2-}. From the Figure, there is an additional peak at – 0.75 V that emerges, which could correspond to another intermediate hat is not present for MoO_4^{2-}; possibly through these reactions:

$$MoO_2 + 2H^+ + e^- \rightarrow Mo^{3+} + 2H_2O \quad (E^o = -0.008\,V)$$

SEM images were taken but were not well resolved however, the EDS data from the Au deposition was taken, there was Mo confirmed at the surface of the gold electrode, for both Mo(VI) and Mo(IV).

(a) 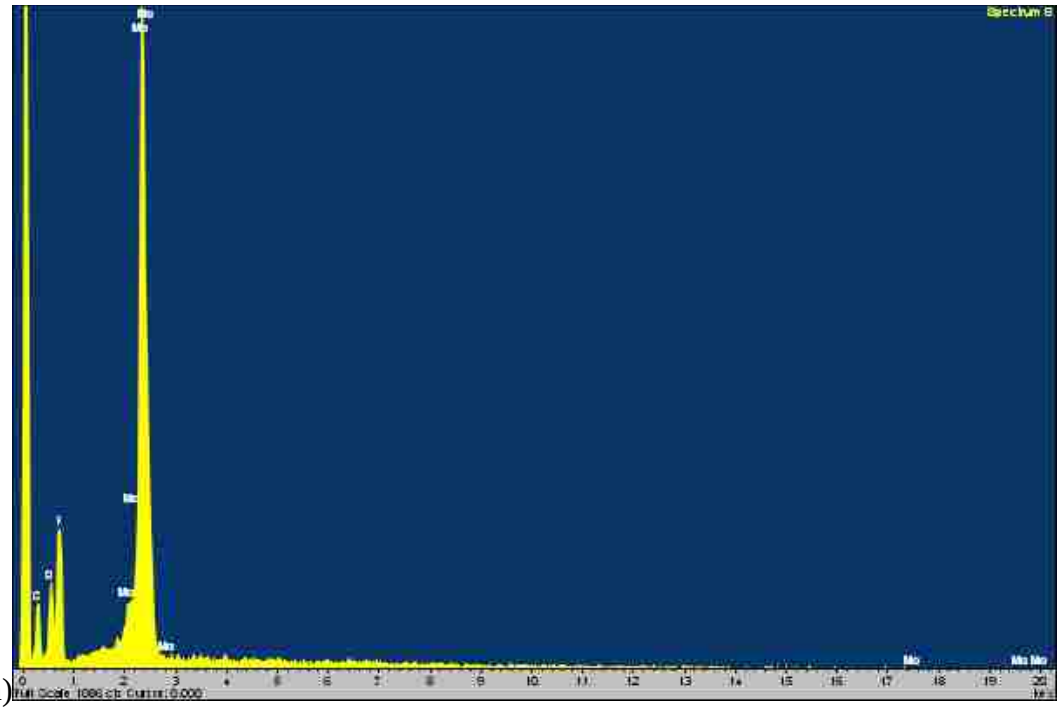

(b) 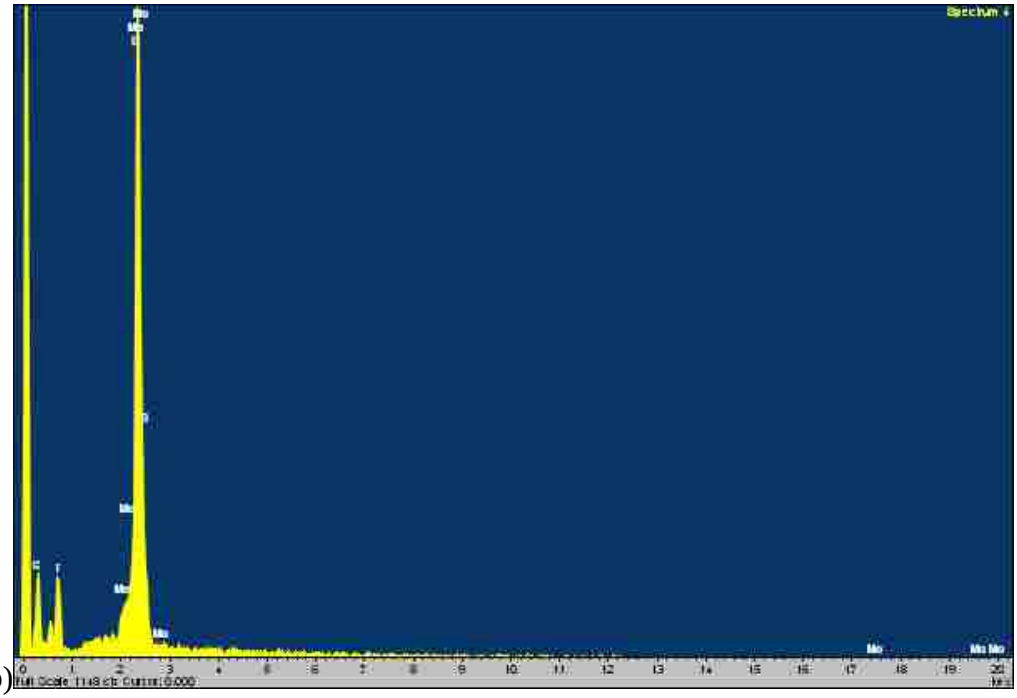

Figure 4.19 a, b: EDS Data for Mo(VI) in HTFSI and Mo(IV) in 0.5 M HTFSI.

The EDS elemental analysis confirms that there is Mo deposited onto the gold surface. There was also an indication of oxygen on the surface, where the scan was taken. The presence of oxygen may be due to the atmospheric exposure, between the time of the experiment and measurements taken. Another source of oxygen may that there was a mixture of Mo metal and Mo oxide deposited onto the gold surface. However, the composition is such that the oxygen content is significantly diminished indicating that there is appreciable Mo metal on the electrodes.

The following Figure (Figure 4.20) is for MoO_4^{2-} dissolved in RTIL with 0.3 M HTFSI in solution on a GC working electrode.

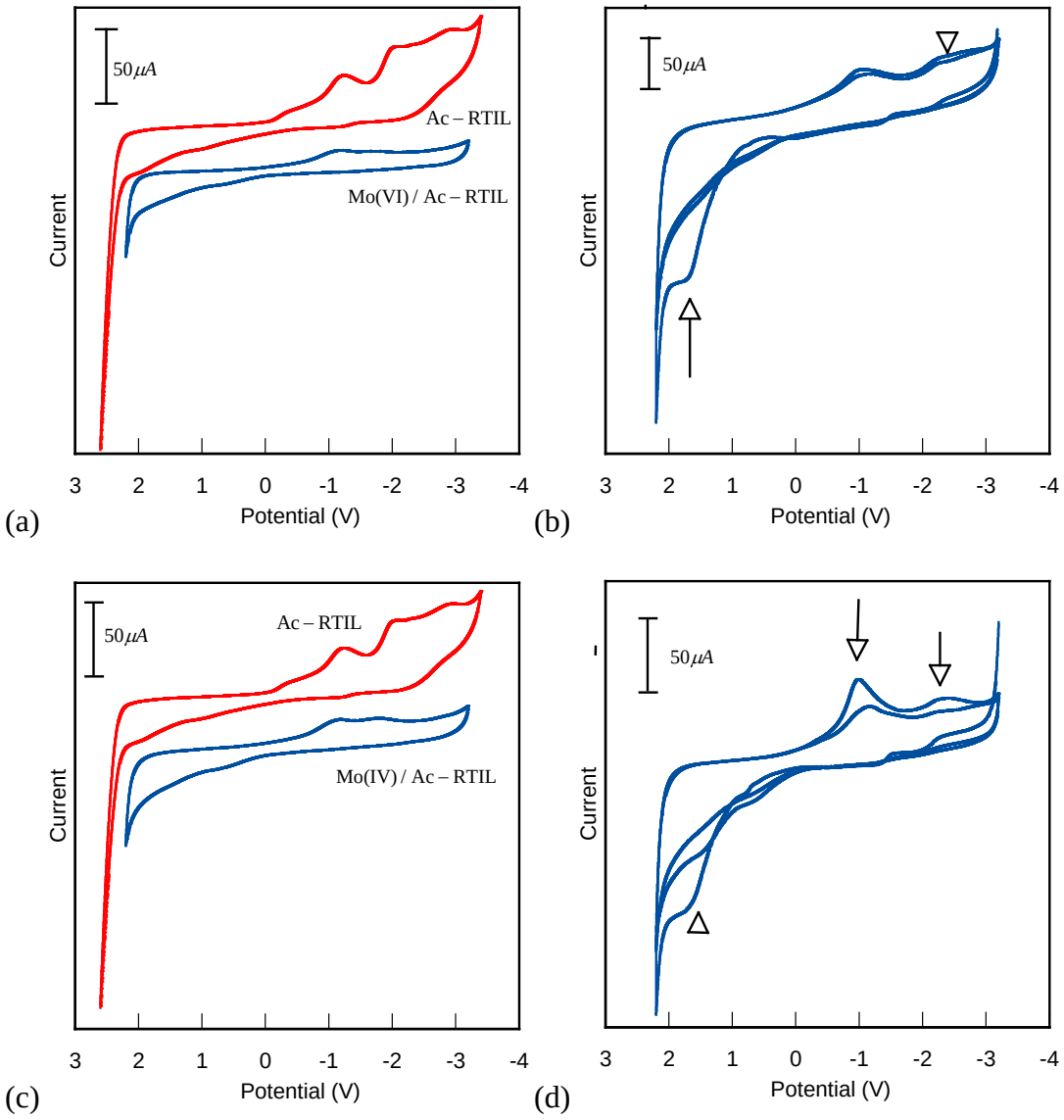

Figure 4.20a, b: Voltammetric response of GC working electrode in solution containing 89 mM MoO_4^{2-} dissolved in RTIL with 0.5 M HTFSI. Figure 4.20a: is the Ac-RTIL background and steady state for Mo(VI) . Figure 4.20b is the progression scans. Figure 4.20c, d: Voltammetric response of GC electrode in a solution containing 89 mM MoO_2 with 0.5 M HTFSI background and steady state. Figure 4.20d is the progression scans of Mo(IV).

In the initial scans (4.20b) there is a broad reduction peak that appears at ~ -2.5 V. This peak is diminished by the time steady state (4.20a) is reached. The addition of H^+ to

the solution for GC improved the voltammetric response. This means adding H^+ aides in the reduction of Mo(VI).

There is a big change in the response between the initial scans (4.20d) and the steady state (4.20c). In the initial scans there are two reduction peaks that emerge at – 1.0 V and a broad peak at – 2.5 V. In the steady state scan the second reduction peak is diminished, which would indicate that there was a change at the GC surface. However, there is an emergence of broad peak at - 1.9 V. The occurrence of the new peak at the steady state could be a result to the change of the surface of the electrode, because if there was no change, then the voltammetric response would stay the same. For the GC electrode the CV with the addition of H^+ (Figure 4.20c) compared to the CV with no HTFSI (Figure 4.16b) has higher electrochemical response with the same concentration of Mo. This would indicate that addition of H^+ into the system for MoO_2, helps the reduction at the GC surface.

Since the mechanism for the electrochemistry occurring at the GC is unknown, the inferences made are based on the electrochemistry for Pt and Au. Since GC is so inert, the possibility of H_{ad} being adsorbed onto the surface is not likely. Therefore, the electrochemical reduction is attributed to the very negative potentials that the GC working electrode can reach. Since there was a change in the voltammetric response, this indicates that there was a change that occurred at the surface of the GC electrode. In these CV's the full potential window was not used, because when it was scanned its maximum window there was no significant electrochemical response.

When analyzing the reduction of MoO_4^{2-} and MoO_2 in RTIL on the different working electrodes there many differences attributed to the working electrode and the solution

composition. Working in a non-aqueous system stabilized both MoO_4^{2-} and MoO_2 relative to the same species in aqueous solution. The addition of HTFSI in RTIL influences the electrochemical reduction of Mo at Pt, Au, and GC surfaces. In some cases the addition of H^+ increased the electrochemical response for the reduction of Mo species while inhibiting the reduction of cations from the RTIL. Although the exact reduction/deposition mechanisms were not established in these studies, clear changes to the electrochemistry where observed with the introduction of H^+ in the RTIL. Furthermore, in contrast to aqueous system the electrochemical processes associated with the reduction and deposition of Mo was achieved using RTIL.

CHAPTER 5

CONCLUSIONS AND FUTURE WORK

5.1 CONCLUSIONS

For the experiments performed in this thesis rhenium was used in place of Tc because of its analogous chemical properties and the lack of available Tc for experimentation. In addition, Re and Tc share the same stable oxidation states which are relevant in the electrochemical analysis and comparison of both species. The reduction mechanisms for the analogous element Re are crucial in understanding the possible reduction mechanisms and recovery of Tc. The solution parameters utilized in these studies were similar to those found in used nuclear fuel containing Tc to ensure continuity and provide real solution parameters. In addition, using solution conditions which typically exist eliminates variability and will aid in future efforts to recover Tc using the methods developed in this thesis.

Developing an understanding the reduction/oxidation of molybdenum is also critical because Tc-99m is obtained from the decay of Mo-99. Approximately 30% Tc-99m is obtained from irradiated Mo-99, while the remainder decays to Tc-99. The residual Tc-99m and eventually Tc-99 remains in the column unused and is discarded as radioactive medical waste. Currently there is no viable procedure in place for increasing the percent elution of Tc-99m from the stream or for the recovery of the Tc-99 from the Mo-99 column. Consequently, understanding the reduction/oxidation of Mo is vital for reclamation purposes.

Prior studies regarding the electrochemical properties of Rhenium investigated the changes secondary to solution parameters including the conjugate bases of acids

including H_2SO_4 and $HClO_4$ with Pt and Au working electrodes. Previous studies indicated that the pH for Re reduction is important; however no definitive study of the influence pH on the reduction mechanism was reported [28]. In addition these studies identified that certain anions (i.e. ClO_4^-, SO_4^{2-}) in solution inhibited the reduction of Re. In addition, it was suggested that the electrochemical reduction of Re at the Pt working electrode is a surface process where surface adsorbed H^+ produces a reducing agent H_2 which enhances the process [28]. These studies also investigated the electrochemical reduction at the Au working electrode. However, Re reduction at Au was not facilitated by the generation of H_2 at the electrode surface and the reduction potential alone was the sole determining factor in the deposition processes.

The pH and solution composition at Pt and Au working electrodes for perrhenate and molybdenum solutions were further investigated in chapter 3 to determine the most efficient method to reduce Re and Mo. The pH of the system was investigated by adding aliquots of NaOH to the ReO_4^- acidic solution. This allowed for the analysis of the changes of pH in targeted Re and Mo reduction. From the experiments performed the pH range for Re reduction was found to be narrow (0.30 to 0.41) and the target pH should be 0.34, shown in Figure 3.1. Furthermore the electrolyte matrix containing NO_3^- did not inhibit the reduction of Re in the solution (i.e. ClO_4^- competitive reduction) as their reduction potentials are different. The pH range for observing the reduction of Re was identified the electrochemical deposition of both species was observed. However, the electrochemical reduction of the species to metal was not achieved in aqueous solution because of competitive reactions in the aqueous environment. Finding the optimum potential window for the Pt working electrode is important for accurate Re reduction. If

the potential $E^o < 0.0$ V, then H_2 is evolved, inhibiting the reduction of the target species. The potential window for the Au working electrode is more negative than that of Pt. Below in Table 5.1 are summarized the potential windows for the aqueous and non-aqueous potential windows for Pt, Au, and GC electrodes.

Table 5.1: Summary of the Potential Windows for Pt, Au, GC in Aqueous and Non-Aqueous Solutions.

Substrate Metal	Aqueous Potential Window	Non-Aqueous Potential Window
Platinum	1.0 V – 0.0 V	1.7 V – (-2.4 V)
Gold	1.0 – (-0.1 V)	1.9 V – (-2.7 V)
Glassy Carbon	N/A	2.6 V – (-2.7 V)

The molybdenum electrochemistry has not been widely studied in aqueous and non-aqueous solutions. Previous studies have suggested that in aqueous solutions Mo(VI) cannot be reduced below Mo(III). In aqueous solutions Mo(VI) becomes Mo(IV) which is its most stable oxidation state inhibiting further reduction. Both Mo(VI) and Mo(IV) form complexes at low pH values, which may influence the electrochemistry and final oxidation state. The deposition of metallic Mo was not achieved using aqueous solutions suggesting that the deposit was in the form of an oxide, MoO_x.

In this thesis, Mo was evaluated with respect to pH, solution conditions and the potential window afforded by the solution and electrode materials utilized. The range of

pH suitable to resolve the reduction of Mo was found to be between 0.11 to 0.38. From the thermodynamic and half-cell potentials, the reduction likely proceeds through MoO_4^{2-} forming MoO_2 consistent with previous studies. At the Pt electrode, the H_{ad} plays the same role in the reduction observed for Re. Likewise, at the Au electrode hydrogen evolution is minimized requiring more negative potentials for the reduction of Mo.

The reduction/oxidation chemistry for Re and Mo were investigated in non-aqueous solutions, RTIL. The RTIL eliminated the confounding side reactions (H_2 and water/metal oxidation). As a consequence of eliminating the side reactions, the potential windows were expanded in order to reach theoretical reduction potentials of Re and Mo. Obtaining the theoretical reduction potentials is vital to reducing Re/Mo/Tc to metal for reclamation purposes, as summarized in Table 5.1. The expansion of the potential window also eliminated the need for H_2 to act as a complimentary reducing agent in the process. The reduction of both Re and Mo at both the Pt and Au working electrode was achieved suggesting that RTIL solutions may be utilized in the reclamation of these species and possibly Tc. These deposits were confirmed by EDS data and found to be reproducibly formed using well defined electrochemical and solutions parameter. These results represent the first targeted reduction of Re and Mo metal from RTIL. The studies presented in this thesis provide the methods and mechanism for the target recovery of Re and Mo. With this knowledge the recovery of Tc from used nuclear fuel and biomedical waste streams can be envisioned.

5.2: Future Work

After the preliminary electrochemical studies Re and Mo reduction and deposition from RTIL solutions very specific questions remain. For example, the concept of "pH"

remains undefined for RTIL solutions. The concept of solvating a proton in ionic liquids is not easily translated into the activity of the species. The definitions that exist for aqueous solutions do not adequately describe or quantify the true value of pH in RTIL. Additional experiments are required to try to define the concept of pH in RTIL. These studies would involve measuring the pH of the RTIL, adding water to the system, sonicating the mixture and allowing the layers to separate, and measuring the pH change in water and RTIL. The change in pH of the water can then be attributed to the H^+ concentration solvated from the RTIL. The decrease in pH of RTIL can then be compared. The changes in pH for both solutions can be plotted and compared to try to elucidate the concept of pH in RTIL solutions.

Additional studies on Re/Mo could involve changing the potential window after the first layers of deposition. The surface of the electrodes change which could result in changes in the electrochemical response, because the potentials windows are optimized for the working electrode not the target species deposited. Finally, taking all of the information gathered from the Re and Mo studies, Tc experiments could be targeted and designed specifically for recovery from used nuclear fuel. A preliminary solubility test was done on a Tc species (tetra-butyl ammonium (TBA)-TcO_4^-) which was fully soluble in the RTIL used. Using all of the information gathered can increase the success rate of recovery and minimize radioactive waste.

APPENDIX A

Ac-RTIL……Acidified Room Temperature Ionic Liquid
Al_2O_3……..…….Alumina
Au……..……..Gold
AuOx……..Gold Oxide
COEX……..Co-Extraction
CV…….Cyclic Voltammetry
E^o……..……Standard Potential
EDS……...……..Energy Dispersive X-ray Spectroscopy
EQCM…….……Electrochemical Quartz Crystal Microbalance
FP……..……..Fission Products
GC……..Glassy Carbon
H_{ad}……...……Adsorbed H
HEU…….High Enriched Uranium
HTFSI……..……Pronotated TFSI
LEU…….……Low Enriched Uranium
LWR……Light Water Reactors
$Me3NPr^+$…….……n-trimethyl-n-propylammonium
Mo…….……..Molybdenum
MOX…….……Mixed Oxide Fuel
Pt…….Platinum
PUREX……..……..Plutonium/Uranium Extraction
Re……Rhenium
ReO_4^-…….Perrhenate
$ReOx_{ad}$……..……..……Adsorbed Rhenium Oxide
RTIL…….……...…Room Temperature Ionic Liquid
SEM……..Scanning Electron Microscope
SCE……...……..Saturated Calomel Electrode
Tc……Technetium
Tc-99……..Technetium Isotope
Tc-99m…….Metastable Technetium
TcO_4^-…….……..……..Pertechnetate
$TFSI^-$…….bis(trifluoromethanesulfonyl) imide
TBP……..tri-n-butyl-phosphate
UNF……..……Used Nuclear Fuel
WE……...……Working Electrode

BIBLIOGRAPHY

1. Benedict, M., *Nuclear Chemical Engineering*. Second ed, ed. T.H. Pigford, Levi, H. 1981: McGraw Hill.
2. Paviet-Hartmann, P., Lineberry, M., Benedict, R., Chap 11: *Nuclear Fuel Reprocessing*. Nuclear Engineering Handbook, ed. K. Kok. 2009: CRS Press.
3. Choppin, G., *Chemical separations in nuclear waste management, the state of the art and alook to the future,*. Institute for the International Cooperative Environmental Research, ed. M.K. Khankhasayev, Plendl, H. S. 2002: Florida State University.
4. NEA, *Actinide separation chemistry in nuclear waste streams and materials*. 1997, NEA/NSC/DOC(97)19, NEA/OECD publication.
5. Sayre, E.D., *Technetium-99*. 1964.
6. Pansters, D. *A Look at La Hague*. 1998 2007 [cited; http://www.ricin.com/nuke/bg/lahague.html].
7. Paviet-Hartmann, P., *Application of crown ethers of technetium 99, iodine 129, and cesium 135 in effluents*, in *Chemistry*. 1992, Université Paris XI: Orsay.
8. Burns, C., Bryan, J., Cotton, F., Ott, K., Kubas, G., Haefner, S., Barrera, J., Hall, K., and Burrell, A., *Technetium Chemistry*, in *LANL Report*. 1996, LANL.
9. Paviet-Hartmann, P., Horkley, J., Pak, J., Brown, E., Todd, T., *Resorcinarenes and aza-crowns as new extractants for the separation of Technetium-99*, in *Scientific Basis for Nuclear Waste Management XXXII MRS Proceedings*, R.B. Rebak, Hyatt, N. C., Pickett, D. A., Editor.
10. Audrieth, L.F., Long, A., Edwards, R. E.,, *Fused Onium Salts as Acids. Reactions in Fused Pyridinium Hydrochloride.* J. Am. Chem. Soc., 1936. **58**(3): p. 428.
11. Crosthwaite, J.M., Muldoon, M. J., Dixon, J. K., Anderson, J. L., and Brennecke, J. F., *Phase transition and decomposition temperatures, heat capacities and viscosities of pyridinium ionic liquids.* J. Chem. Thermodyn., 2005. **37**(6): p. 559-568.
12. MacFarlane, D.R., Golding, J., Forsyth, S., and Deacon, G.B., *Low Viscosity ionic liquids based on organic salts of the dicynamide anion.* Chem. Commun., 2001. **16**: p. 1430.
13. Zhang, S., Lu, X., Zhou, Q., Li, X., *Ionic Liquids = physiochemical properties*. 2009: Elsevier.
14. Plieth, W., *Electrochemistry for materials science*. 2008: Elsevier.
15. Rogers, R., Seddon, K., *Ionic liquids- Solvents of the future*. 2003. **31**: p. 792-793.
16. Senentz, G., Drain, F., Baganz, C., *COEX ^{TM} Recycling Plant: A New Standard for An Integrated Plant, Proceedings Global*. 2009: Paris, France, Sept 6-11, 2009.
17. Drain, F., Emin, J. L., Vinoche, R., Baron, P., *COEX Proces: Cross bredding etween innovation and industrial experience, Proceedings Waste Management 2008.* 2008: Phoenix, AZ, Feb 2008.
18. Gray, L.W., *From separations to reconstitution- A short history of plutonium in the U.S. and Russia*, in *LLNL report*. 1999. UCRL-JC-133802.
19. Hylko, J.M. *How to Solve the Used Nuclear Fuel Storage Problem*. [http://www.usnuclearenergy.org/HYLKO.htm] 2008 .

20. Nelson, T.O., James, C. A., Kolman, D. G., *The United States Pit Disassembly and conversion project meeting the MOX fuel Specification*, in *LANL Report*. 1998. LAUR-98-2936.
21. Yoshihara, K. and T. Omori, *Technetium in the environment*, in *Technetium and Rhenium Their Chemistry and Its Applications*. 1996, Springer Berlin / Heidelberg. p. 17-35.
22. Anders, E., *The radiochemistry of technetium*, in *Nuclear Science Series*. 1960, National Academy of Sciences.
23. Schwochau, K., *Technetium and Radiopharmaceutical Applications*. 2000: Wiley-VCH.
24. Fried, S., Jaffey, A.H., Hall, N.F., Glendenin, L.E., *Half-Life of the Long Lived Tc-99.* Physical Review, 1951. **81**(5): p. 741-747.
25. Emsley, J., *Nature's Building Blocks: An A-Z Guide to the Elements*. 2001, Oxford, England: Oxford University Press.
26. Thomas, G., Maddahi, J., *The Technetium Shortage.* Journal of Nuclear Cardiology, 2010.
27. National Research Council of the National Academies, *Medical Isotope Production Without Highly Enriched Uranium*. 2009, Washington, D.C.: The National Academies Press.
28. Mendez, E.C., Maria; Luna, Ana; Zinola, Carlos; Kremer, Carlos; Martins, Maria., *Electrochemical behavior of aqueous acid perrhenate-containing solutions on noble metals: critical review and new experimental evidence.* Journal of Colloid and Interface Science, 2003. **263**: p. 119-132.
29. Kremer, C., Dominguez, S., Perez-Sanchez, M., Mederos, A., Kremer, E., *Comparative Electrochemistry of Technetium (V) and Rhenium (V) Dioxo Complexes.* J.Radioanal. Nucl. Chem., Letters, 1996. **213**(4): p. 263-274.
30. Bard, A., Faulkner, *Electrochemical Methods: Fundamentals and Applications*, ed. Harris. 2001: John Wiley & Sons, Inc.: pp. 5, 23-26, 227, 231, 419, 581, 591
31. Bard, A.J., Parsons, Roger; Jordan, Joseph, *Standard Potentials in Aqueous Solution*. 1985, New York: Marcel Kekker, Inc.
32. Goldstein, J., Newbury, D., Joy, D., Lyman, C., Achlin, P., Lifshin, E., Sawyer, L., and Michael, J. *Scanning Electron Microscopy and X-Ray Microanalysis*. 2003: Springer.: pp. 21-22, 195-197
33. Verhoeven, J., *Scanning Electron Microscopy*. 1986. ASM Handbook. Vol. 10
34. Bell, D.C., Garratt, A. J., *Energy dispersive X-ray analysis in the electron microscope*. Microscopy Handbooks. 2003: BIOS Scientific Publishers, Ltd.
35. Kikuchi, S., *Electrodeposition of Rhenium from Perchloric Acid Solution.* Journal of the Nation Chemical Laboratory for Industry, 1986. **81**(9): p. 473-476.
36. Kremer, C., Dominguez, S., Perez-Sanchez, M., Mederos, A., Kremer, E., *Comparative Electrochemistry of Technetium (V) and Rhenium (V) Dioxo Complexes.* J.Radioanal. Nucl. Chem., Letters, 1996. **213**(4): p. 263-274.
37. Kikuchi, S., *Electrodeposition of Rhenium from Perchloric Acid Solution.* Journal of the National Chemical Laboratory for Industry, 1986. **81**(9): p. 473-476.
38. Han, B.M., Alan; Stevenson, Keith, *Electrochemical Deposition and Characterization of Mixed-Valent Rhenium Oxide Films Prepared from a Perrhenate Solution.* American Chemical Society, 2007. **23**: p. 10837-10845.

39. Atkins, H.L., *Radiopharmaceuticals kits*, in *report BNL*. 1973 NEED REPORT NUMBER.
40. Harris, D., *Quantitative Chemical Analysis*. 6th ed. 2003: W.H. Freeman & Co.: pp. 145-145, 147, 254.
41. Pitzer, K., Peiper, J. C., *Activity Coefficient of Aqueous $NaHCO_3$.* Journal Of Phys. Chem., 1979(84): p. 2396-2398.
42. Janata, J., Zuman, P., *Electrochemical Acidity Functions.* Collect. Czech. Chem. Commun., 2010. **74**: p. 1635-1646.

VITA

Graduate College
University of Nevada, Las Vegas

Pauline N. Serrano

Degree:

Bachelor of Science, Biochemistry, 2005
University of Nevada, Las Vegas

Special Honors and Awards:

Chemistry Representative – UNLV College of Sciences Graduate Council
Chemistry Representative – Dean's College of Sciences Undergraduate Committee
Member – Gold Key International Honor Society

Thesis Title: Electrochemistry of Technetium Analogues Rhenium and Molybdenum in Room Temperature Ionic Liquid

Thesis Examination Committee:

Chairperson, David Hatchett, Ph.D.
Committee Member, Dong-Chan Lee, Ph.D.
Committee Member, Patricia Paviet-Hartmann, Ph.D.
Graduate Faculty Representative, Jaci Batista, Ph.D.